Circulation Journal
Official Journal of the Japanese Circulation Society
http://www.j-circ.or.jp

ORIGINAL ARTICLE
Pediatric Cardiology and Adult Congenital Heart Disease

Inhibition of Phosphodiesterase Type 3 Dilates the Rat Ductus Arteriosus Without Inducing Intimal Thickening

Yasuhiro Ichikawa, MD; Utako Yokoyama, MD, PhD; Mari Iwamoto, MD, PhD; Jin Oshikawa, MD, PhD; Satoshi Okumura, MD, PhD; Motohiko Sato, MD, PhD; Shumpei Yokota, MD, PhD; Munetaka Masuda, MD, PhD; Toshihide Asou, MD, PhD; Yoshihiro Ishikawa, MD, PhD

Background: Prostaglandin E_1 (PGE_1), via cAMP, dilates the ductus arteriosus (DA). For patients with DA-dependent congenital heart disease (CHD), PGE_1 is the sole DA dilator that is used until surgery, but PGE_1 has a short duration of action, and frequently induces apnea. Most importantly, PGE_1 increases hyaluronan (HA) production, leading to intimal thickening (IT) and eventually DA stenosis after long-term use. The purpose of this study was therefore to investigate potential DA dilators, such as phosphodiesterase 3 (PDE3) inhibitors, as alternatives to PGE_1.

Methods and Results: Expression of PDE3a and PDE3b mRNAs in rat DA tissue was higher than in the pulmonary artery. I.p. milrinone (10 or 1 mg/kg) or olprinone (5 or 0.5 mg/kg) induced maximal dilatation of the DA lasting for up to 2 h in rat neonates. In contrast, vasodilation induced by PGE_1 (10 μg/kg) was diminished within 2 h. No respiratory distress was observed with milrinone or olprinone. Most important, milrinone did not induce HA production, cell migration, or proliferation when applied to cultured rat DA smooth muscle cells. Further, high expression of both PDE3a and PDE3b was demonstrated in the human DA tissue of CHD patients.

Conclusions: Because PDE3 inhibitors induced longer-lasting vasodilation without causing apnea or HA-mediated IT, they may be good alternatives to PGE_1 for patients with DA-dependent CHD. (*Circ J* 2012; **76:** 2456–2464)

Key Words: Congenital heart disease; Ductus arteriosus; Milrinone; Phosphodiesterase

The ductus arteriosus (DA), the fetal arterial connection between the pulmonary artery (PA) and the descending aorta, is essential to maintain fetal life in utero. The DA closes after birth by 2 different mechanisms: vasoconstriction and intimal thickening (IT).[1–3] During the first few hours after birth, acute vasoconstriction occurs as a result of smooth muscle contraction in the DA. This is triggered by increased oxygen tension, due to the initiation of spontaneous breathing, and decreased circulating prostaglandin E_2 (PGE_2), due to disconnection from the placenta.[3] This functional vasoconstriction, however, must be preceded by IT of the DA, because vascular remodeling, including IT, is critical for anatomical closure of the DA.

The IT of the DA is a result of many cellular processes, such as an increase in smooth muscle cell (SMC) migration and proliferation, the production of hyaluronan (HA) under the endothelial layer, and decreased elastin fiber assembly.[1,3,4] We have previously demonstrated that PGEs promoted HA production via cAMP/protein kinase A and subsequent SMC migration, resulting in IT of the DA during the late gestational period.[1,4,5] In patients with DA-dependent congenital heart disease (CHD), such as pulmonary atresia with intact ventricular septum or arch anomalies (coarctation of aorta or interruption of aortic arch), however, patent DA after birth is essential for survival.

PGE_1 is widely used to keep the DA open because it increases intracellular cAMP and thus dilates the DA. But PGE_1 induces HA-mediated IT and thus DA stenosis after prolonged use.[6] The fact that it induces only a very short duration of vasodilation, together with its severe adverse effects, such as apnea, respiratory distress, and hypotension, present additional problems, making it difficult for some patients with CHD to

Received February 16, 2012; revised manuscript received May 10, 2012; accepted June 4, 2012; released online July 6, 2012 Time for primary review: 13 days

Cardiovascular Research Institute (Y. Ichikawa, U.Y., S.O., M.S., Y. Ishikawa), Department of Pediatrics (Y. Ichikawa, M.I., S.Y.), Medical Science and Cardiorenal Medicine (J.O.), Department of Surgery (M.M.), Yokohama City University, Yokohama; and Department of Cardiovascular Surgery, Kanagawa Children's Medical Center, Yokohama (T.A.), Japan

Mailing address: Utako Yokoyama, MD, PhD or Yoshihiro Ishikawa, MD, PhD, Cardiovascular Research Institute, Yokohama City University, 3-9 Fukuura, Kanazawa-ku, Yokohama 236-0004, Japan. E-mail: utako@yokohama-cu.ac.jp or yishikaw@med.yokohama-cu.ac.jp

ISSN-1346-9843 doi:10.1253/circj.CJ-12-0215

continue the use of PGE_1 until surgery. As such, possible alternatives to PGE_1 need to be investigated.

Phosphodiesterases (PDEs), which catalyze the hydrolysis of cAMP/cGMP, constitute a superfamily of at least 11 gene families (PDE1–PDE11).[7] The 2 PDE3 subfamilies, PDE3A and PDE3B, are encoded by closely related genes,[8] and both hydrolyze cAMP. PDE3 inhibitors have been approved by the US Food and Drug Administration (FDA) for use as vasodilators as well as in heart failure. Two of these are milrinone and olprinone, which are widely used to treat heart failure[9–12] and persistent pulmonary hypertension in neonates.[13,14] Previous studies have shown that the PDE3 inhibitors milrinone, amrinone, and cilostazol counteract indomethacin-induced DA contraction.[15,16] Thus, PDE3 inhibitors alone may be sufficient to dilate the DA. Nevertheless, it remains undetermined whether they induce IT, which is a major problem with PGE_1, via HA production, cell migration, or cell proliferation. In the current study, we investigated the role of PDE3 inhibitors in DA vascular remodeling and vasodilation with a view to their potential use as alternatives to the current PGE therapy.

Methods

Animals and Materials

Timed pregnant Wistar rats were purchased from Japan SLC (Hamamatsu, Japan). All animal studies were approved by the institutional animal care and use committees of Yokohama City University. Milrinone, platelet derived growth factor-BB (PDGF-BB), 3-[4,5-dimethylthiazol-2-yl]-2,5-diphenyltetrazolium bromide (MTT), trichloroacetic acid, and 10% buffered formalin were obtained from Wako (Osaka, Japan). Olprinone, cilostazol, rolipram, PGE_1, PGE_2, elastase type II, trypsin inhibitor, bovine serum albumin V, poly-L-lysine, penicillin-streptomycin solution, acetic anhydride, triethylamine, Dulbecco's modified Eagle's medium (DMEM), and Hank's balanced salt solution (HBSS) were purchased from Sigma-Aldrich (St Louis, MO, USA). Collagenase II was purchased from Worthington Biochemical (Lakewood, NJ, USA). Collagenase/dispase was purchased from Roche Diagnostics (Tokyo, Japan). Fetal bovine serum (FBS) was purchased from Equitech-Bio (Kerrville, TX, USA).

Primary Culture of Rat SMCs

Vascular SMCs in primary culture were obtained from the DA (DASMCs), the aorta (ASMCs), and the PAs (PASMCs) of Wistar rats on the 21st day of gestation. Isolation of DASMCs and ASMCs has been described previously.[17] To obtain PASMCs, the branch extralobular PAs were dissected, cleaned from adherent tissue, and cut into small pieces. The tissues were transferred to a 1.5-ml centrifuge tube that contained 800 μl of collagenase-dispase enzyme mixture (1.5 mg/ml collagenase-dispase, 0.5 mg/ml of elastase type II-A, 1 mg/ml of trypsin inhibitor type I-S, and 2 mg/ml of bovine serum albumin fraction V in HBSS). Digestion was carried out at 37°C for 15 min. Cell suspensions were then centrifuged, and the medium was changed to a collagenase II enzyme mixture (1 mg/ml collagenase II, 0.3 mg/ml trypsin inhibitor type I-S, and 2 mg/ml bovine serum albumin fraction V in HBSS). After 12 min of incubation at 37°C, cell suspensions were transferred to growth medium in 35-mm poly-L-lysine-coated dishes in a moist tissue culture incubator at 37°C in 5% CO_2-95% ambient mixed air. The growth medium contained DMEM with 10% FBS, 100 U/ml penicillin, and 100 mg/ml streptomycin. We confirmed that >99% of cells were positive for α-smooth muscle actin and exhibited typical hill-and-valley morphology. Expression of PDE3, prostaglandin E receptor EP4 (EP4), and prostacyclin (IP) receptor mRNAs in DASMCs, ASMCs, and PASMCs is shown in Figure S1.

Table. Patient Characteristics

Patient no.	Age at operation	Diagnosis
1	0 days	Asplenia, PA, TAPVD, CA, SV
2	1 day	Asplenia, CoA, CA, SV
3	2 days	IAA, Aorticopulmonary window
4	2 days	CoA, VSD
5	3 days	TGA, CoA
6	4 days	CoA, VSD
7	13 days	CoA, VSD
8	1 month	HypoLV, CoA, VSD

CA, common atrium; CoA, coarctation of the aorta; hypoLV, hypoplastic left ventricle; IAA, interruption of aortic arch; PA, pulmonary atresia; SV, single ventricle; TAPVD, total anomalous pulmonary venous drainage; TGA, transposition of the great arteries; VSD, ventricular septal defect.

Human Tissue From CHD Patients

We obtained 8 neonatal DAs and adjacent aortas during cardiac surgery in children between 0 days and 1 month of age. All excised tissue was fixed in 4% paraformaldehyde within 3 h. The DA tissues were obtained from the Yokohama City University Hospital and Kanagawa Children's Medical Center. The study was approved by the human subject committees at both Yokohama City University and Kanagawa Children's Medical Center. Detailed patient information is summarized in Table.

RNA Isolation and Quantitative Reverse Transcription-Polymerase Chain Reaction (RT-PCR)

Pooled vascular tissues were obtained from Wistar rats on the 21st day of gestation. After excision, tissues were frozen in liquid nitrogen and stored at −80°C. The total RNA was isolated from the tissues using an RNeasy Mini Kit (Qiagen, Valencia, CA, USA) according to the manufacturer's instructions and from the cultures using Trizol reagent (Invitrogen, Carlsbad, CA, USA). The primers were designed based on the rat nucleotide sequences of PDE3a (NM_017337) (5'-CGC CTG AGA AGA AGT TTG C-3' and 5'-AGA CAG CAT AGG ACG AAG TGA AG-3'), PDE3b (NM_017229.1) (5'-TCC AAA GCA GAG GTC ATC ATC-3' and 5'-GTA TCA AGA AAT CCT ACG GGT GA-3'), EP4 (NR_032076.3) (5'-CTC GTG GTG CGA GTG TTC AT-3' and 5'-AAG CAA TTC TGA TGG CCT GC-3'), and IP (NM_00177644.1) (5'-GGG CAC GAG AGG ATG AAG-3' and 5'-GGG CAC ACA GAC AAC ACA AC-3'). RT-PCR was performed using a PrimeScript RT reagent Kit (TaKaRa Bio, Tokyo, Japan) and real-time PCR was performed using SYBR Green (Applied Biosystems, Foster City, CA, USA). The abundance of each gene was determined relative to that in 18S ribosomal RNA.

Rapid Whole-Body Freezing Method

To study the in situ morphology and inner diameter of the neonatal DA, a rapid whole-body freezing method was used as previously described.[2] Fetuses on the 21st day of gestation were delivered by cesarean section, and immediately after birth i.p. injections of milrinone (10 mg/kg, 1 mg/kg, 0.1 mg/kg), olprinone (5 mg/kg, 0.5 mg/kg, 0.05 mg/kg), or PGE_1 (10 μg/kg) were given. The rat pups were frozen in liquid nitrogen at 0,

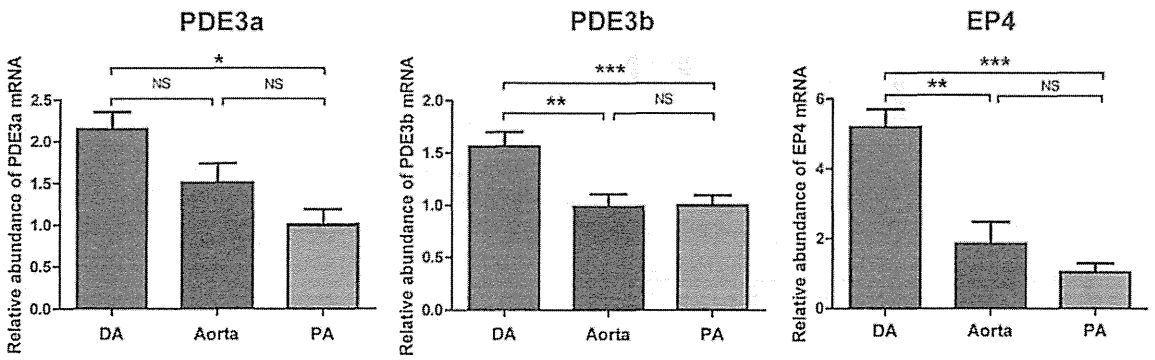

Figure 1. Quantitative reverse transcription-polymerase chain reaction (RT-PCR) of PDE3a, PDE3b, and EP4 in rat ductus arteriosus (DA), aorta, and pulmonary artery (PA) tissue on the 21st day of gestation. n=4–5. *P<0.05; **P<0.01; ***P<0.001. PDE, phosphodiesterase; NS, not significant.

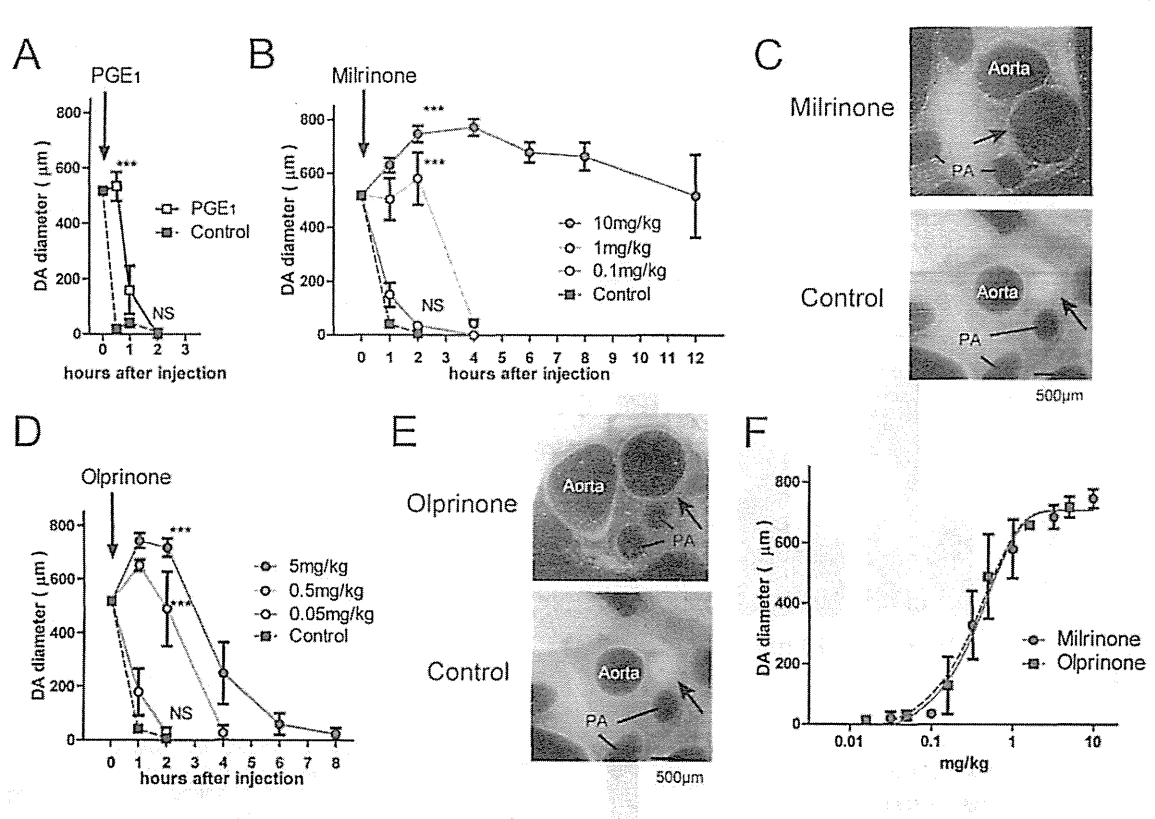

Figure 2. Effects of milrinone and olprinone on vasodilation of the ductus arteriosus (DA) as observed using the rapid whole-body freezing method. (A) Prostaglandin E_1 (PGE_1; 10μg/kg)-induced dilation of rat DA (n=4–6). (B) Vasodilatory effect of milrinone on rat DA. Rat neonates were injected i.p. with milrinone (n=4–6). (C) Representative images of rat DAs treated with 10mg/kg of milrinone or saline (control) for 2h using the whole-body freezing method (arrow). (D) Vasodilatory effect of milrinone on rat DA. Rat neonates were injected i.p. with olprinone (n=4–6). (E) Representative images of rat DAs treated with 5mg/kg of olprinone or control for 2h using the whole-body freezing method (arrow). (F) Milrinone or olprinone dilated DA in a dose-dependent manner. Vasodilatory effects of phosphodiesterase 3 (PDE3) inhibitors were examined 2h after injection (n=4–6). ***P<0.001 and NS vs. control. NS, not significant.

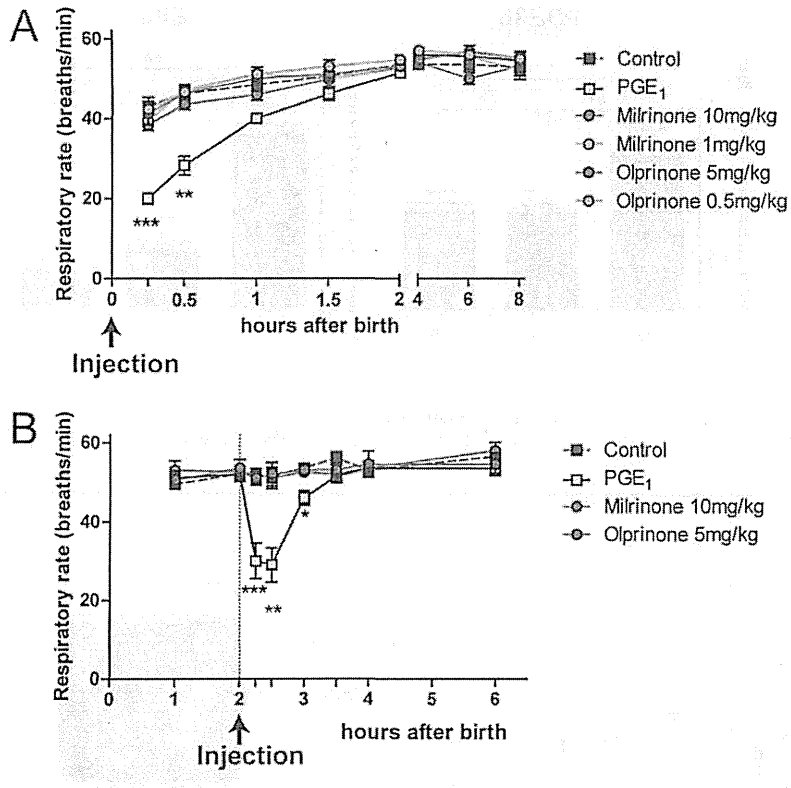

Figure 3. Effects of phosphodiesterase 3 (PDE3) inhibitors and prostaglandin E_1 (PGE_1) on respiratory distress. (A) Respiratory rate of rat neonates given each drug immediately after birth, the same as in Figure 2 (n=6–9). (B) Respiratory rate of rat neonates given each drug 2h after birth (n=4). *P<0.05, **P<0.01 and ***P<0.001 vs. control. No mark, not significant vs. control.

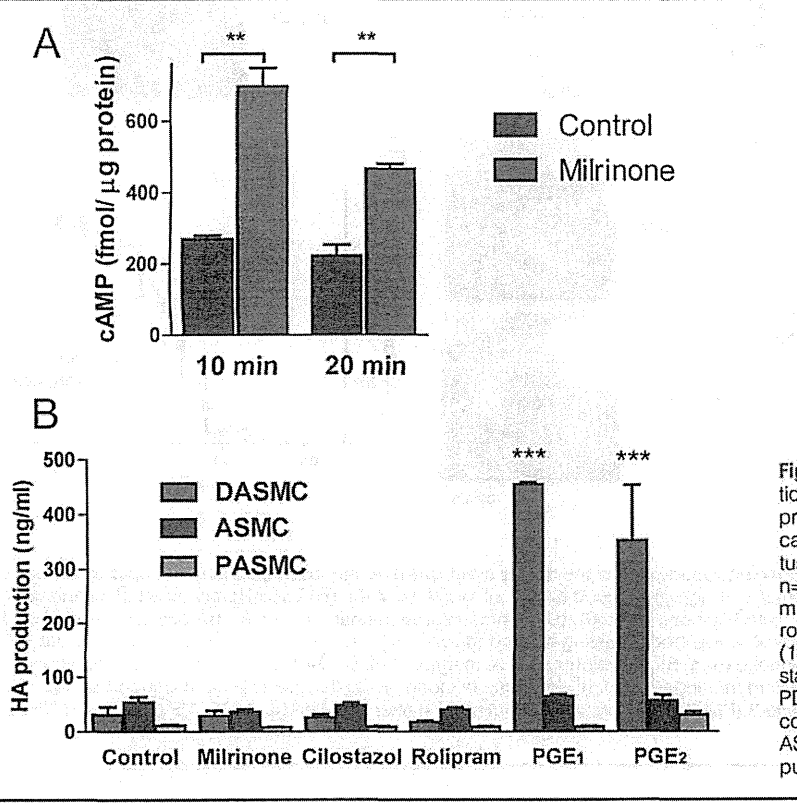

Figure 4. Milrinone increased cAMP production, but it did not induce hyaluronan (HA) production. (A) Milrinone (10 μmol/L) significantly increased cAMP accumulation in ductus arteriosus smooth muscle cells (DASMCs; n=4). (B) HA production in SMCs treated with milrinone (10 μmol/L), cilostazol (10 μmol/L), rolipram (10 μmol/L), prostaglandin (PG)E_1 (1 μmol/L), or PGE_2 (1 μmol/L; n=4–6). Cilostazol, phosphodiesterase 3 (PDE3); Rolipram, PDE4 inhibitor. **P<0.01 and ***P<0.001 vs. control. No mark, not significant vs. control. ASMCs, aortic smooth muscle cells; PASMCs, pulmonary artery smooth muscle cells.

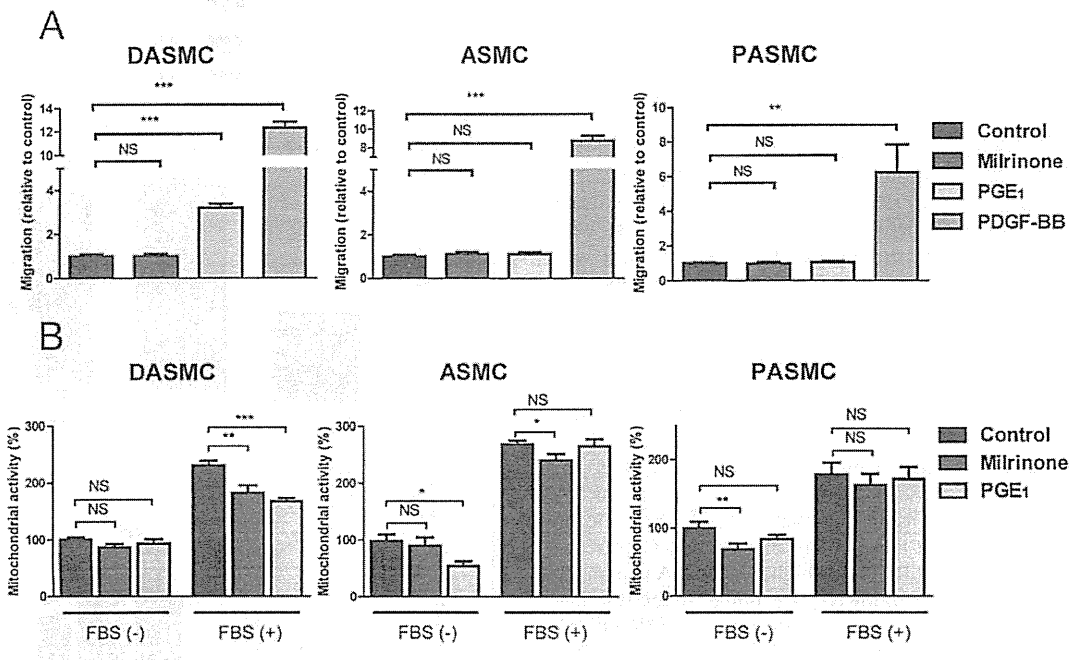

Figure 5. Milrinone did not promote migration and proliferation in smooth muscle cells (SMCs). (A) Migration of SMCs treated with milrinone (10 μmol/L), prostaglandin E1 (PGE1; 1 μmol/L), or platelet derived growth factor-BB (PDGF-BB; 10 ng/ml) using the Boyden chamber method (n=4–5). (B) Proliferation of SMCs treated with milrinone (10 μmol/L) or PGE1 (1 μmol/L) in the presence of 0 or 10% fetal bovine serum (FBS) on MTT assay (n=5–9). *P<0.05, **P<0.01 and ***P<0.001. NS, not significant. ASMCs, aortic smooth muscle cells; DASMCs, ductus arteriosus smooth muscle cells; PASMCs, pulmonary artery smooth muscle cells.

0.5, 1, 2, 4, 6, 8, and 12 h after injection. The frozen thoraxes were then cut on a microtome, and the inner diameter of each DA was measured.

Determination of Respiratory Rate

Fetuses on the 21st day of gestation were delivered by cesarean section, and at 0 or 2 h after birth i.p. injections of milrinone (10 mg/kg, 1 mg/kg), olprinone (5 mg/kg, 0.5 mg/kg), or PGE1 (10 μg/kg) were given. We measured the respiratory rate by counting the movements of the rat thorax.

Quantification of HA

The amount of HA in the cell culture supernatant was measured according to the latex agglutination method as previously described.[1]

SMC Migration Assay

The migration assay was performed using 24-well transwell culture inserts with polycarbonate membranes (8-μm pores; Corning, Corning, NY, USA) as previously described.[1] Cells were stimulated with milrinone (10 μmol/L), PGE1 (1 μmol/L), PDEF-BB (10 ng/ml), HA (200 ng/ml), or milrinone+HA for 3 days.

Cell Proliferation Assay

SMCs were cultured on 24-well plates at 1×10^5 cells per well in DMEM supplemented with 10% FBS. After various treatments over 3 days, 500 μl of 1 mg/ml MTT solution was added to each well and incubated for 2 h. The supernatants were aspirated, and the formazan crystals in each well were solubilized with 0.05 mol/L HCl (500 μl). Each solution (100 μl) was placed in a 96-well plate. SMC proliferation was measured based on absorbance at 570 nm using a microplate reader.

Immunohistochemistry

Immunohistochemical analysis was performed as previously described.[1,18] Rabbit polyclonal anti-PDE3A antibody (sc-20792) and goat polyclonal anti-PDE3b antibody (sc-11835) were purchased from Santa Cruz Biotechnology (Santa Cruz, CA, USA). A color extraction method using BIOREVO bz-9000 (KEYENCE, Osaka, Japan) was performed to quantify the expression of PDE3 s in the DAs and the aortas of patients 1, 4, 5, and 8 (Table). Eighteen fields in the smooth muscle layer of the DA and the aorta respectively were examined in 4 cases. On diaminobenzidine staining, PDE3a-positive or PDE3b-positive areas were extracted and counted on the screen.

Radioimmunoassay Measurement of Cyclic AMP Production

Measurement of cAMP accumulation in DASMCs was performed as previously described.[2,19] Briefly, DASMCs grown on 24-well plates were serum-starved for 24 h and assayed for cAMP production after a 10- or 20-min period of incubation with 10 μmol/L of milrinone. Reactions were terminated by aspiration of the media and the addition of 300 μl of ice-cold trichloroacetic acid (7.5%) to each well. Forty microliters of each sample were acetylated and incubated with ^{125}I-cAMP (Perkin Elmer, Waltham, MA, USA) and 50 μl of rabbit anti-cAMP antibody (diluted 1:3,000, Millipore, Billerica, MA, USA) overnight at 4°C. Each mixture was then incubated with

50 μl of goat anti-rabbit antibody with magnetic beads (Qiagen) for 1 h. Separation of bound antibodies from free antibodies was achieved by filtration, and bound radioactivity was counted. Production of cAMP was normalized to the amount of protein per sample.

Statistical Analysis

Data are presented as mean±SEM of independent experiments. Statistical analysis was performed between 2 groups using unpaired 2-tailed Student's t-test or unpaired t-test with Welch's correction, and among multiple groups using 1-way analysis of variance followed by Tukey's multiple comparison test. $P<0.05$ was considered significant.

Results

Messenger RNA of PDE3 Isoforms Highly Expressed in Rat DA

We first examined whether the target molecule of PDE3 inhibitors is highly expressed in the DA. We measured the mRNA expression of PDE3s using quantitative RT-PCR in the rat DA, aorta, and PA on the 21st day of gestation (Figure 1). Expression of PDE3a mRNA was higher in the DA than in the PA. Expression of PDE3b mRNA was higher in the DA than in the aorta or the PA. We also confirmed that EP4 mRNA was more highly expressed in the DA than in the aorta or the PA. Thus, PDE3 isoforms were abundantly expressed in the DA relative to the PA.

Vasodilatory Effects of PDE3 Inhibitors on Rat DA In Vivo

PDE3 inhibitors are widely used in neonates and children with low cardiac output following myocarditis and cardiovascular surgery for CHD.[20,21] We examined whether milrinone or olprinone dilated the DA using the rapid whole-body freezing method in rat neonates. Neonates were injected with 1 of these drugs immediately after birth to mimic the vasodilatory treatment currently used in DA-dependent CHD.

I.p. injection of PGE_1 (10 μg/kg, the amount that is given i.v. daily as a clinical maintenance dose) induced maximum dilatation of the DA for 30 min, but this effect was completely lost within 2 h after injection (Figure 2A). A single i.p. injection of 10 mg/kg of milrinone maintained maximum dilation of the DA for up to 12 h (Figures 2B,C); 1 mg/kg of milrinone, the amount that is given i.v. daily as a clinical maintenance dose, maintained maximum dilatation for 2 h, after which DA closure occurred at 4 h after injection. And 0.1 mg/kg of milrinone did not affect DA tone. Both 5 mg/kg and 0.5 mg/kg of olprinone, the latter of which is suitable for daily i.v. use as a clinical maintenance dose, induced maximum dilatation for 1 h after injection (Figures 2D,E). A dose of 0.05 mg/kg olprinone did not dilate the DA. Thus, both milrinone and olprinone produced dose-dependent vasodilatory effects (Figure 2F), but those of milrinone lasted longer.

PDE3 Inhibitors Do Not Induce Respiratory Distress

Given that respiratory distress is a major adverse effect of PGE_1,[22] we examined whether PDE3 inhibitors cause respiratory distress. We measured the respiratory rate of rat neonates given milrinone, olprinone, or PGE_1. When rat neonates were given each drug immediately after birth, PGE_1 significantly reduced the respiratory rate at 15 or 30 min after injection, *whereas* milrinone (1 and 10 mg/kg) and olprinone (0.5 and 5 mg/kg) did not induce respiratory distress up to 8 h after injection compared to the saline control (Figure 3A). To exclude the possibility that neonates given PGE_1 had a congenital respiratory problem, we examined the effect of drugs using a different injection timing. We confirmed that all rat neonates had established normal breathing 1 h after birth, and then each drug was given. PGE_1 significantly reduced the respiratory rate up to 1 h after injection. In contrast, milrinone (10 mg/kg) and olprinone (5 mg/kg) did not affect the respiratory rate compared to the control (Figure 3B). These data suggest that PDE3 inhibitors did not cause respiratory distress.

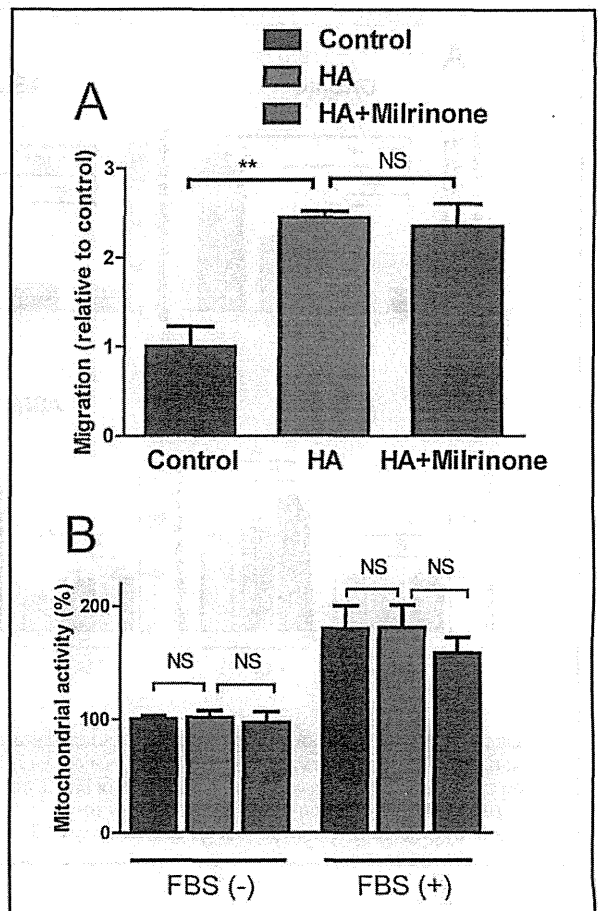

Figure 6. Effect of co-treatment of hyaluronan (HA) with milrinone on migration and proliferation in ductus arteriosus smooth muscle cells (DASMCs). (A) Migration of SMCs with co-treatment of HA (200 ng/ml) and milrinone (10 μmol/L) using the Boyden chamber method (n=4–5). (B) Proliferation of SMCs with co-treatment of HA (200 ng/ml) and milrinone (10 μmol/L) in the presence of 0 or 10% fetal bovine serum (FBS) on MTT assay (n=8). **P<0.01. NS, not significant.

Milrinone Do Not Promote HA Production or SMC Migration and Proliferation

Although it was previously suggested that PDE3 inhibitors induced vasodilation of the DA, it remained unknown whether they also induced IT formation, a key process in the anatomical closure of the DA. It is known that PGEs stimulate HA production along with increased DASMC migration through the action of HA as a potent trigger of cell migration. This is the major mechanism underlying the increase in IT induced by PGEs.[1,2,5]

We thus examined whether a PDE3 inhibitor, milrinone,

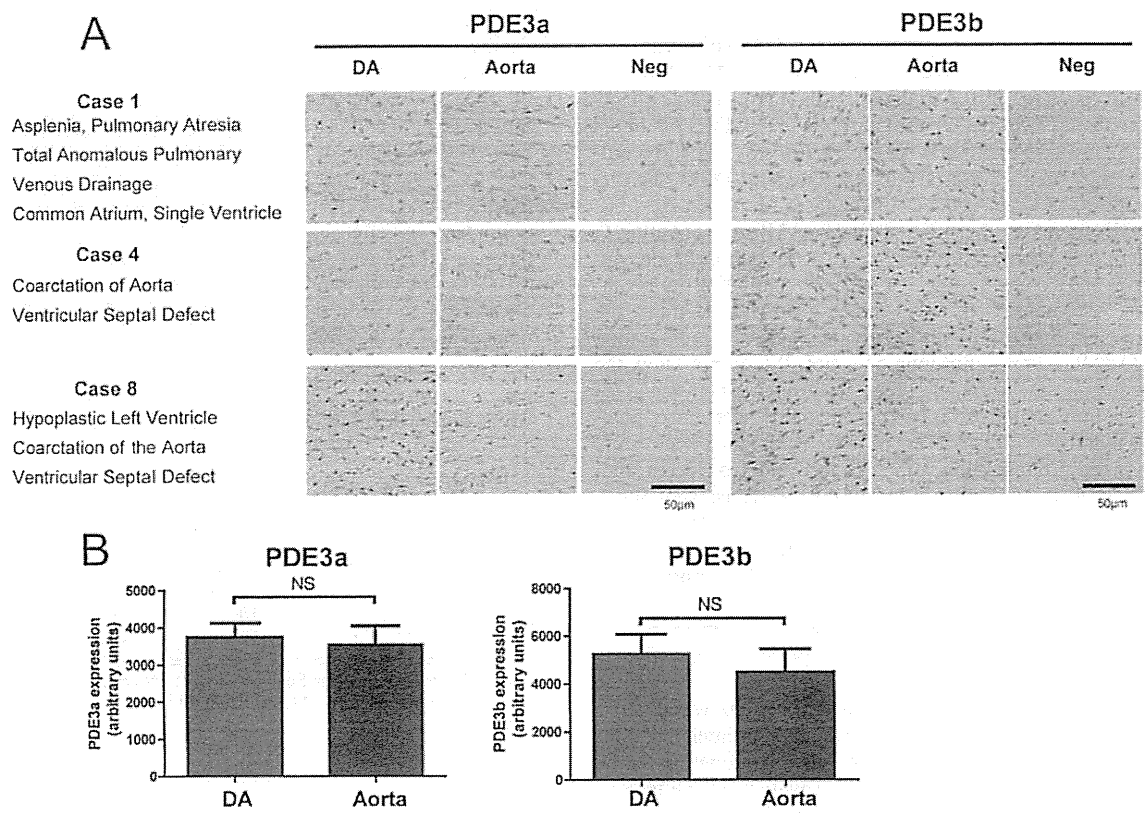

Figure 7. (A) Representative images of immunoreaction to PDE3a and PDE3b in the human ductus arteriosus (DA) and aortic smooth muscle layers according to type of congenital heart disease. No immunoreaction was detected when omitting the primary antibody, as in PDE3a Neg and PDE3b Neg. (B) Quantification of PDE3a and PDE3b in the DA and the aorta using a color extraction method (n=4). PDE, phosphodiesterase; NS, not significant.

regulated HA production or SMC migration. First, we confirmed cAMP production in the presence of milrinone. Milrinone significantly increased cAMP accumulation in DASMCs at a dosage of 10 μmol/L, which also induced marked dilatation of DA explants (Figure 4A).[16] But the same dosage of milrinone (10 μmol/L) did not induce HA production in DASMCs (Figure 4B). We also confirmed that the PDE3 inhibitor cilostazol did not induce HA production in DASMCs. Similarly, PGE_1 (1 μmol/L) induced DASMC migration; but milrinone did not increase DASMC migration, as determined using the Boyden chamber method (Figure 5A). The cells used for these tests were sufficiently stimulated with PGE_1 to induce HA production and with PDGF-BB to induce migration. Next, we examined the effects of a PDE3 inhibitor on SMC proliferation, because SMC proliferation plays a role in IT formation of the DA.[23,24] Milrinone and PGE_1 did not increase DASMC proliferation, as determined on MTT assay, in the presence of 0 or 10% FBS (Figure 5B). Moreover, we found that milrinone did not enhance HA-mediated migration in DASMCs (Figure 6A). Milrinone also did not affect proliferation in HA-treated DASMCs (Figure 6B). Similarly, in ASMCs and PASMCs, neither milrinone nor PGE_1 increased HA production or cell migration and proliferation (Figures 4B,5). These findings suggest that PDE3 inhibitors do not promote HA production or cell migration or proliferation, although they do produce cAMP and dilate the DA.

PDE3a and PDE3b Highly Expressed in the Smooth Muscle Layer in Human DA Tissue

The expression pattern of PDE3s in human DA remains unknown. We examined PDE3a and PDE3b protein expression in the DA of 8 patients with CHD, such as interruption of the aortic arch, complex aortic coarctation, hypoplastic left ventricle, and asplenia. The DA of all patients had a strong immunoreaction for both PDE3a and PDE3b (Figure 7A). It has been demonstrated that PDE3a and PDE3b are abundantly expressed in the rat and human aorta.[25,26] The expression of PDE3a and PDE3b in the DAs was equivalent to that in the adjacent aortas (Figure 7B). This demonstrates that PDE3s are abundantly expressed in human patients with CHD of the type that may require long-term vasodilatotherapy prior to surgery.

Discussion

The present study has demonstrated that the PDE3 inhibitors milrinone and olprinone dilate the DA without causing apnea and have a longer duration of action than PGE_1. These findings are expected to apply to human patients, given that PDE3s are abundantly expressed in the DA tissue of infants

with CHD. Importantly, this study has shown for the first time that these PDE3 inhibitors do not promote HA production, cell migration, and cell proliferation in the DASMC, processes that potently induce IT and thus DA closure.[1] The PDE3 inhibitors are very unlikely to produce these unfavorable effects when used as DA dilators. Furthermore, these PDE3 inhibitors are already used in humans for other purposes.[9,10,13,14] Accordingly, they may serve as useful alternatives to PGE1, the current means of keeping the DA patent.

PGE1 increases the production of cAMP by activating G protein and adenylyl cyclase.[1,2,27] In contrast, milrinone increases the concentration of cAMP by inhibiting its breakdown.[7] Although both drugs increase cAMP and dilate the DA, PGE1 induces HA production and subsequent migration in DASMCs while milrinone does not. We do not know the molecular mechanism underlying this difference between PGE1 and the PDE inhibitors. It can be tentatively speculated, however, that they differ in terms of intracellular localization and thus in terms of coupling with other molecules, as recent studies have suggested.[28] Regardless of the mechanisms involved, it is known that PGE1 and PGE2 both increase cAMP production and induce HA production via increased expression of HA synthase 2,[1,5] and we found that a PDE4 inhibitor, rolipram, did not induce HA production (Figure 4B). Alternatively, increases in cGMP, which is also induced by milrinone, may play a role. These issues need to be further investigated in future studies.

Previous studies effectively demonstrated the vasodilatory effects of the PDE3 inhibitors milrinone, amrinone and cilostazol on the rat or sheep DA that underwent contraction by indomethacin.[15,16] In contrast, we have evaluated the effects of PDE3 inhibitors in the absence of indomethacin to examine the effects of PDE3 inhibitors in more relevant clinical settings. We also found, for the first time, that olprinone, a relatively new PDE3 inhibitor, dilates the DA. The present finding that these PDE3 inhibitors do not increase HA production is also novel, because this question had not been investigated previously.

The present study shows that milrinone does not induce SMC migration and proliferation in the DA (Figures 5,6). The present findings are, at least in part, consistent with those obtained using vascular SMCs from non-DA vessels. PDE3 inhibitors have elsewhere been shown to reduce proliferation and migration of vascular SMCs and to decrease the accumulation of synthetic/activated vascular SMCs in the intimal layers of damaged blood vessels.[7,29,30] Similarly, in peripheral PAs, PDE3 and PDE4 inhibition do not promote PASMC migration.[31] Furthermore, PDE3a deficiency caused G0/G1 cell cycle arrest in PDE3a knockout mice.[8]

PGE1 is currently the sole DA dilator, but PGE1-induced apnea or respiratory distress was noted in 18% of patients with CHD.[32] Respiratory depression was particularly common in infants weighing <2.0 kg at birth who received PGE1 therapy (42%).[22] The present study showed that milrinone and olprinone did not induce respiratory distress in rat neonates (Figure 3). Furthermore, no occurrence of apnea or respiratory distress due to PDE3 inhibitors has been previously reported.[9,10,13,14] Therefore, the PDE3 inhibitors are very unlikely to produce an unfavorable effect on respiration when used as DA dilators. It should be noted that PDE3 inhibitors have adverse effects, such as arrhythmia or hypotension.[33] Milrinone reduces the risk of low cardiac output syndrome for some pediatric patients after congenital heart surgery, but milrinone use is an independent risk factor for clinically significant tachyarrhythmias.[34] Although it was not feasible to examine arrhythmias and change in blood pressure in rat neonates in this study, careful further study is warranted to examine adverse effects.

It should be emphasized that both the PDE3a protein and the PDE3b protein were abundantly detected in the smooth muscle layer and the IT layer in all human DA samples tested, regardless of diagnosis or patient age at the time of operation (Figure 7). A previous study demonstrated that PDE3 inhibitors prevented DA closure in premature infants with persistent pulmonary hypertension.[15,35,36] Together with these findings, those of the present study suggest that PDE3 inhibitors can dilate the DA without inducing IT, and that they may serve as alternatives to PGE1, the current DA vasodilator used for patients with DA-dependent CHD.

Acknowledgment

We are grateful to Yuka Sawada for excellent technical assistance.

Disclosure

This work was supported by grants from the Ministry of Health, Labor, and Welfare of Japan, a Grant-in-Aid for Scientific Research on Innovative Areas (22136009 to Y. Ishikawa and 23116541 to U. Yokoyama), the Ministry of Education, Culture, Sports, Science, and Technology of Japan (Y. Ichikawa, U. Yokoyama, M. Masuda and Y. Ishikawa), the Kitsuen Kagaku Research Foundation (Y. Ishikawa), the Yokohama Foundation for Advanced Medical Science (Y. Ichikawa and U. Yokoyama), the Takeda Science Foundation (U. Yokoyama and Y. Ishikawa), the Miyata Cardiac Research Promotion Foundation (U. Yokoyama), and the Mochida Memorial Foundation for Medical and Pharmaceutical Research (U. Yokoyama).

References

1. Yokoyama U, Minamisawa S, Quan H, Ghatak S, Akaike T, Segi-Nishida E, et al. Chronic activation of the prostaglandin receptor EP4 promotes hyaluronan-mediated neointimal formation in the ductus arteriosus. *J Clin Invest* 2006; **116:** 3026–3034.
2. Yokoyama U, Minamisawa S, Katayama A, Tang T, Suzuki S, Iwatsubo K, et al. Differential regulation of vascular tone and remodeling via stimulation of type 2 and type 6 adenylyl cyclases in the ductus arteriosus. *Circ Res* 2010; **106:** 1882–1892.
3. Smith GC. The pharmacology of the ductus arteriosus. *Pharmacol Rev* 1998; **50:** 35–58.
4. Yokoyama U, Minamisawa S, Ishikawa Y. Regulation of vascular tone and remodeling of the ductus arteriosus. *J Smooth Muscle Res* 2010; **46:** 77–87.
5. Sussmann M, Sarbia M, Meyer-Kirchrath J, Nusing RM, Schror K, Fischer JW. Induction of hyaluronic acid synthase 2 (HAS2) in human vascular smooth muscle cells by vasodilatory prostaglandins. *Circ Res* 2004; **94:** 592–600.
6. Mitani Y, Takabayashi S, Sawada H, Ohashi H, Hayakawa H, Ikeyama Y, et al. Fate of the "opened" arterial duct: Lessons learned from bilateral pulmonary artery banding for hypoplastic left heart syndrome under the continuous infusion of prostaglandin E1. *J Thorac Cardiovasc Surg* 2007; **133:** 1653–1654.
7. Maurice DH, Palmer D, Tilley DG, Dunkerley HA, Netherton SJ, Raymond DR, et al. Cyclic nucleotide phosphodiesterase activity, expression, and targeting in cells of the cardiovascular system. *Mol Pharmacol* 2003; **64:** 533–546.
8. Begum N, Hockman S, Manganiello VC. Phosphodiesterase 3A (PDE3A) deletion suppresses proliferation of cultured murine vascular smooth muscle cells (VSMCs) via inhibition of mitogen-activated protein kinase (MAPK) signaling and alterations in critical cell cycle regulatory proteins. *J Biol Chem* 2011; **286:** 26238–26249.
9. Klein L, O'Connor CM, Leimberger JD, Gattis-Stough W, Pina IL, Felker GM, et al. Lower serum sodium is associated with increased short-term mortality in hospitalized patients with worsening heart failure: Results from the Outcomes of a Prospective Trial of Intravenous Milrinone for Exacerbations of Chronic Heart Failure (OPTIME-CHF) study. *Circulation* 2005; **111:** 2454–2460.
10. Niemann JT, Garner D, Khaleeli E, Lewis RJ. Milrinone facilitates resuscitation from cardiac arrest and attenuates postresuscitation myocardial dysfunction. *Circulation* 2003; **108:** 3031–3035.
11. Greenberg B. Acute decompensated heart failure: Treatments and challenges. *Circ J* 2012; **76:** 532–543.

12. Thomas SS, Nohria A. Hemodynamic classifications of acute heart failure and their clinical application: An update. *Circ J* 2012; **76:** 278–286.
13. Bassler D, Choong K, McNamara P, Kirpalani H. Neonatal persistent pulmonary hypertension treated with milrinone: Four case reports. *Biol Neonate* 2006; **89:** 1–5.
14. Bassler D, Kreutzer K, McNamara P, Kirpalani H. Milrinone for persistent pulmonary hypertension of the newborn. *Cochrane Database Syst Rev* 2010; **(11):** CD007802.
15. Toyoshima K, Momma K, Imamura S, Nakanishi T. In vivo dilatation of the fetal and postnatal ductus arteriosus by inhibition of phosphodiesterase 3 in rats. *Biol Neonate* 2006; **89:** 251–256.
16. Liu H, Manganiello V, Waleh N, Clyman RI. Expression, activity, and function of phosphodiesterases in the mature and immature ductus arteriosus. *Pediatr Res* 2008; **64:** 477–481.
17. Yokoyama U, Minamisawa S, Adachi-Akahane S, Akaike T, Naguro I, Funakoshi K, et al. Multiple transcripts of Ca2+ channel alpha1-subunits and a novel spliced variant of the alpha1C-subunit in rat ductus arteriosus. *Am J Physiol Heart Circ Physiol* 2006; **290:** H1660–H1670.
18. Akaike T, Jin MH, Yokoyama U, Izumi-Nakaseko H, Jiao Q, Iwasaki S, et al. T-type Ca2+ channels promote oxygenation-induced closure of the rat ductus arteriosus not only by vasoconstriction but also by neointima formation. *J Biol Chem* 2009; **284:** 24025–24034.
19. Yokoyama U, Patel HH, Lai NC, Aroonsakool N, Roth DM, Insel PA. The cyclic AMP effector Epac integrates pro- and anti-fibrotic signals. *Proc Natl Acad Sci USA* 2008; **105:** 6386–6391.
20. Hoffman TM, Wernovsky G, Atz AM, Kulik TJ, Nelson DP, Chang AC, et al. Efficacy and safety of milrinone in preventing low cardiac output syndrome in infants and children after corrective surgery for congenital heart disease. *Circulation* 2003; **107:** 996–1002.
21. Taoka M, Shiono M, Hata M, Sezai A, Iida M, Yoshitake I, et al. Child with fulminant myocarditis survived by ECMO Support: Report of a child case. *Ann Thorac Cardiovasc Surg* 2007; **13:** 60–64.
22. Lewis AB, Freed MD, Heymann MA, Roehl SL, Kensey RC. Side effects of therapy with prostaglandin E1 in infants with critical congenital heart disease. *Circulation* 1981; **64:** 893–898.
23. Tananari Y, Maeno Y, Takagishi T, Sasaguri Y, Morimatsu M, Kato H. Role of apoptosis in the closure of neonatal ductus arteriosus. *Jpn Circ J* 2000; **64:** 684–688.
24. Boudreau N, Rabinovitch M. Developmentally regulated changes in extracellular matrix in endothelial and smooth muscle cells in the ductus arteriosus may be related to intimal proliferation. *Lab Invest* 1991; **64:** 187–199.
25. Reinhardt RR, Chin E, Zhou J, Taira M, Murata T, Manganiello VC, et al. Distinctive anatomical patterns of gene expression for cGMP-inhibited cyclic nucleotide phosphodiesterases. *J Clin Invest* 1995; **95:** 1528–1538.
26. Palmer D, Maurice DH. Dual expression and differential regulation of phosphodiesterase 3A and phosphodiesterase 3B in human vascular smooth muscle: Implications for phosphodiesterase 3 inhibition in human cardiovascular tissues. *Mol Pharmacol* 2000; **58:** 247–252.
27. Breyer RM, Bagdassarian CK, Myers SA, Breyer MD. Prostanoid receptors: Subtypes and signaling. *Annu Rev Pharmacol Toxicol* 2001; **41:** 661–690.
28. Houslay MD. Underpinning compartmentalised cAMP signalling through targeted cAMP breakdown. *Trends Biochem Sci* 2010; **35:** 91–100.
29. Netherton SJ, Jimmo SL, Palmer D, Tilley DG, Dunkerley HA, Raymond DR, et al. Altered phosphodiesterase 3-mediated cAMP hydrolysis contributes to a hypermotile phenotype in obese JCR: LA-cp rat aortic vascular smooth muscle cells: Implications for diabetes-associated cardiovascular disease. *Diabetes* 2002; **51:** 1194–1200.
30. Souness JE, Hassall GA, Parrott DP. Inhibition of pig aortic smooth muscle cell DNA synthesis by selective type III and type IV cyclic AMP phosphodiesterase inhibitors. *Biochem Pharmacol* 1992; **44:** 857–866.
31. Pullamsetti S, Krick S, Yilmaz H, Ghofrani HA, Schudt C, Weissmann N, et al. Inhaled tolafentrine reverses pulmonary vascular remodeling via inhibition of smooth muscle cell migration. *Respir Res* 2005; **6:** 128.
32. Meckler GD, Lowe C. To intubate or not to intubate? Transporting infants on prostaglandin E1. *Pediatrics* 2009; **123:** e25–e30.
33. Shin DD, Brandimarte F, De Luca L, Sabbah HN, Fonarow GC, Filippatos G, et al. Review of current and investigational pharmacologic agents for acute heart failure syndromes. *Am J Cardiol* 2007; **99:** 4A–23A.
34. Smith AH, Owen J, Borgman KY, Fish FA, Kannankeril PJ. Relation of milrinone after surgery for congenital heart disease to significant postoperative tachyarrhythmias. *Am J Cardiol* 2011; **108:** 1620–1624.
35. Yasuda K, Koyama N, Nomura T, Suzuki Y. Effects of phosphodiesterase 3 inhibitors to premature PDA. *J Jpn Soc Prem Newborn Med* 2004; **16:** 395 (in Japanese).
36. Nakamura M, Yamanouchi T, Taguchi T, Suita S. Effect of phosphodiesterase III inhibitor on persistent pulmonary hypertension of neonate associated with congenital diaphragmatic hernia: A case report. *J Jpn Soc Pediatr Surg* 2001; **37:** 1073–1077 (in Japanese).

Supplementary Files

Supplementary File 1

Figure S1. Quantitative RT-PCR of PDE3a, PDE3b, EP4 and IP in the DASMCs, ASMCs, PASMCs.

Please find supplementary file(s);
http://dx.doi.org/10.1253/circj.CJ-12-0215

J Pharmacol Sci 119, 381 – 389 (2012)

Journal of Pharmacological Sciences

Full Paper

Pharmacological Stimulation of Type 5 Adenylyl Cyclase Stabilizes Heart Rate Under Both Microgravity and Hypergravity Induced by Parabolic Flight

Yunzhe Bai[1], Takashi Tsunematsu[1], Qibin Jiao[1], Yoshiki Ohnuki[2], Yasumasa Mototani[2], Kouichi Shiozawa[2], Meihua Jin[1], Wenqian Cai[1], Hui-Ling Jin[1], Takayuki Fujita[1], Yasuhiro Ichikawa[1], Kenji Suita[1], Reiko Kurotani[1,3], Utako Yokoyama[1], Motohiko Sato[1], Kousaku Iwatsubo[4], Yoshihiro Ishikawa[1,4], and Satoshi Okumura[1,2,*]

[1]*Cardiovascular Research Institute, Yokohama City University Graduate School of Medicine, Yokohama 236-0004, Japan*
[2]*Department of Physiology, Tsurumi University School of Dental Medicine, Yokohama 230-8501, Japan*
[3]*Biochemical Engineering, Faculty of Engineering, Yamagata University, Yonezawa, Yamagata 992-8501, Japan*
[4]*Cardiovascular Research Institute, Department of Cell Biology & Molecular Medicine and Medicine (Cardiology), New Jersey Medical School of UMDNJ, Newark, New Jersey 07103, USA*

Received April 25, 2012; Accepted June 21, 2012

Abstract. We previously demonstrated that type 5 adenylyl cyclase (AC5) functions in autonomic regulation in the heart. Based on that work, we hypothesized that pharmacological modulation of AC5 activity could regulate the autonomic control of the heart rate under micro- and hypergravity. To test this hypothesis, we selected the approach of activating AC5 activity in mice with a selective AC5 activator (NKH477) or inhibitor (vidarabine) and examining heart rate variability during parabolic flight. The standard deviation of normal R-R intervals, a marker of total autonomic variability, was significantly greater under micro- and hypergravity in the vidarabine group, while there were no significant changes in the NKH477 group, suggesting that autonomic regulation was unstable in the vidarabine group. The ratio of low frequency and high frequency (HF) in heart rate variability analysis, a marker of sympathetic activity, became significantly decreased under micro- and hypergravity in the NKH477 group, while there was no such decrease in the vidarabine group. Normalized HF, a marker of parasympathetic activity, became significantly greater under micro- and hypergravity in the NKH477 group. In contrast, there was no such increase in the vidarabine group. This study is the first to indicate that pharmacological modulation of AC5 activity under micro- and hypergravity could be useful to regulate the autonomic control of the heart rate.

Keywords: adenylyl cyclase isoform, autonomic nerve activity, parabolic flight, heart rate variability, microgravity

Introduction

Cardiac function is regulated by the autonomic nervous system. Sympathetic regulation leads to coupling of the β-adrenergic receptor (β-AR) and Gs, the G-protein responsible for stimulating activity of adenylyl cyclase (AC), a membrane-bound enzyme that catalyzes the conversion of ATP to cyclic AMP (cAMP), thereby stimulating protein kinase A (PKA) and ultimately increasing cardiac contractility and heart rate (HR) (1 – 5). Parasympathetic regulation counteracts these effects through the activation of the muscarinic receptor and Gi, the G-protein that can inhibit cardiac contractility and heart rate (6). The autonomic nervous system constitutes the two arms of regulation in the heart. We developed a mouse model with disruption of a major AC isoform (type 5) in the heart and demonstrated that type 5 AC (AC5) regulates cardiac function through the parasympa-

*Corresponding author. okumura-s@tsurumi-u.ac.jp
Published online in J-STAGE on July 31, 2012 (in advance)
doi: 10.1254/jphs.12102FP

thetic arm of the autonomic nervous system, as well as through the sympathetic arm (7 – 9).

The autonomic nervous system is known to be altered under microgravity (10) and hypergravity (11, 12). We have previously examined the role of AC5 in the regulation of the autonomic nervous system in the heart under micro- and hypergravity induced by parabolic flights using transgenic mouse models with AC5 overexpressed in the heart (AC5TG) or with disrupted AC5 (AC5KO) and analyzed heart rate variability during parabolic flight. Changes in heart rate variability (HRV) in response to micro- and hypergravity were augmented in AC5KO, but attenuated in AC5TG, suggesting that AC5 plays an important role in stabilizing heart rate control via autonomic regulation under gravitational stress (13).

We hypothesized that pharmacological regulation of AC5 activity could modulate the autonomic control of the heart rate under gravitational stress during parabolic flight. To test this hypothesis, we decided to examine the effect on HRV of activating or inhibiting AC5 activity in wild-type mice with a selective AC5 activator: 6-[3-(dimethylamino)propionyl]forskolin (NKH477) (14) or an AC5 inhibitor: vidarabine (15) during parabolic flight. We found that HR was stabilized by increasing AC5 activity with NKH477, but destabilized by decreasing AC5 activity with vidarabine under micro- and hypergravity during parabolic flight, in accordance with our previous findings using AC5TG and AC5KO.

We also examined the the ratio between low frequency (LF) and high frequency (HF), a marker of sympathetic activity, and normalized HF (nHF), a marker of parasympathetic activity during the parabolic flight and found that AC5 activity plays an important role to show continuous responses in these autonomic parameters such as LF/HF or nHF, under micro- and hypergravity (16).

Many astronauts suffer to varying degrees from symptoms suggestive of autonomic dysfunction such as nausea, vomiting, and dizziness during the early days of space flight (17), as well as showing severe orthostatic intolerance for several days after spaceflight (18, 19). The underlying molecular mechanism and appropriate treatment for the autonomic dysfunction in space and on earth after space flight remain unknown. However, not only trained astronauts but also normal subjects will stay in space in the near future. Thus, it is important to clarify the mechanism and to establish suitable treatment of autonomic dysfunction during and after spaceflight. This study is the first to demonstrate that pharmacological activation/inhibition of AC5 activity can regulate the autonomic control of the heart rate under micro- and hypergravity, indicating the importance of regulating AC5 activity for the treatment of autonomic dysfunction in space and on earth after spaceflight.

Materials and Methods

Parabolic flight experiment

Parabolic flight experiments were performed in a jet airplane operated by the Diamond Air Service in Nagoya using the same protocol previously employed by us (13). Briefly, in one parabolic flight, which lasted for approximately 1 h, 8 – 12 parabolas were performed in total with a 4 – 6-min interval between consecutive parabolas. At the end of each parabolic flight, mice were euthanized by cervical dislocation and replaced with the next mice. Parabolic flight was divided into five phases (Fig. 1). The first phase (I) was in normogravity (1 G, G: gravity), the second phase (II) was in hypergravity (1.3 G), the third phase (III) was in microgravity (0.03 G), the fourth phase (IV) was in hypergravity (1.8 G), and the fifth phase (V) was in normogravity (1 G). Each parabola provided 15 – 20 s of microgravity (phase III) and hypergravity (phase IV) and we evaluated data from the first parabola, except in Figs. 3B, 4B, 5B, 6B, in which the G force in the hypergravity phase (phase II) before the microgravity phase was kept below 1.3 G to avoid excessive gravity stress on mice and the effect of previous parabolas. During the experiment, the temperature in the plane was kept at 22°C ± 2°C and air pressure was 0.9 ± 0.1 atm.

Animals

Male C57BL/6CrSlc mice aged 4 months were used for this experiment (Japan SLC, Inc., Hamamatsu). The

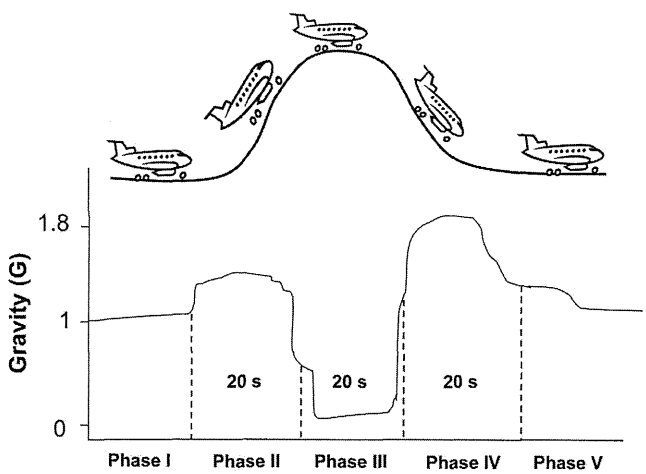

Fig. 1. Schematic representation of parabolic flight. Each parabola provided approximately 20 s of 0.03 G (G; gravity). Parabolic flight was divided into five phases. The first phase (I) was normogravity (1 G), the second phase (II) was hypergravity (1.3 G), the third phase (III) was microgravity (0.03 G), the fourth phase (IV) was hypergravity (1.8 G), and the fifth phase (V) was normogravity (1 G). The Y-axis indicates changes in gravity.

care and treatment of the animals were carried out according to the Japanese Government Animal Protection and Management Law (no. 105) and the Guidelines for Animal Experiments of Yokohama City University School of Medicine.

Experimental design and protocol

ECG recordings were obtained with a telemetric unit (PhysioTel; Data Sciences International, St. Paul, MN, USA). Infusion of NKH477 (1 $mg \cdot kg^{-1} \cdot day^{-1}$) (14), vidarabine (15 $mg \cdot kg^{-1} \cdot day^{-1}$) (15), or phosphate-buffered saline (PBS) as a control was done via an osmotic minipump (Model 2001; ALZET, Cupertino, CA, USA), which was implanted 16 h before the parabolic flight.

Time-domain measures

Conscious mice were separately placed in double-walled plastic cages, which were placed on a receiver in a special rack within the aircraft, and data from the freely moving mice were recorded by the data acquisition system during flight, as described previously by us (13). HRV measurements included mean HR, R-R interval (mean, max, minimum) and the standard deviation of normal R-R intervals (SDNN). The different G phases causes important changes in the R-R interval. Therefore, we also used the coefficient of variation (CV, %) as a normalized index of SDNN (CV-SDNN). SDNN (ms) = SD of all normal R-R intervals; CV-SDNN (%) = SDNN / mean R-R × 100.

Frequency-domain measures

In the frequency domain, the power spectral density was calculated by applying the fast Fourier transformation (FFT) to overlapping segments of the resampled data and by averaging the spectral results (16, 20). The FFT was calculated by using 512 points and half overlap with a Hann window. Cutoff frequencies divided the power spectrum into two main parts, LF (0.4 – 1.5 Hz) and HF (1.5 – 4.0 Hz) powers and were determined by multiplying the standard frequencies used in human studies by 10 to account for HR differences between mice and humans, as recommended by Gehrmann et al. (21). HF powers were normalized to account for differences in total power (TP) between animals by multiplying the power region of interest by 100 and dividing by the difference between TP and very LF power (0.0 – 0.4 Hz) (16).

Statistical analyses

All data are reported as the mean ± S.E.M. Statistical comparisons were performed with the Kruskal-Wallis nonparametric test followed by the Dunn test (Figs. 2, 3, 7, 8). Differences were considered significant at $P < 0.05$.

Results

Effect of parabolic flight on HR

Mean HR in the NKH477, vidarabine, and control groups were evaluated in each phase of parabolic flight during the first parabola. The HR in phase I in the NKH477 group was significantly higher than that in the control group [control group (n = 12): 558 ± 81 vs. NKH477 group (n = 8): 681 ± 38 bpm; $P < 0.01$] (Fig.

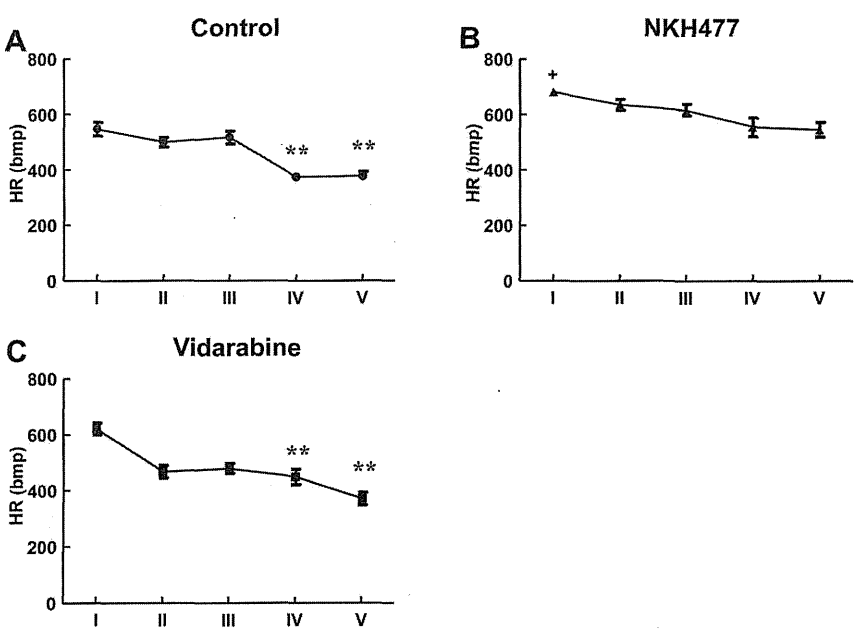

Fig. 2. Comparison of HR during parabolic flights. Comparison of HR among phases I, II, III, IV, and V in the control (n = 12) (A), NKH477 (n = 8) (B), vidarabine (n = 8) (C) groups during the first parabola. HR was compared between phase I and phase II, III, IV, or V in each group (**$P < 0.01$) and also between the control and NKH477 groups ($^{+}P < 0.05$).

2B), as previously found in AC5TG (13, 22). HR showed a significant decrease in later phases (IV – V) in the control and vidarabine groups, but there was no significant change in the NKH477 group, suggesting that HR was stabilized in the NKH477 group, compared with the other groups during parabolic flight.

Effect of parabolic flight on R-R interval of HRV

Maximum, mean, and minimum R-R intervals in the three groups were examined during the first and eighth parabolas (Fig. 3). Maximum, mean, and minimum R-R intervals, in general, increased gradually in later phases (I through IV) during the first parabola (Fig. 3A). When maximum, mean, and minimum R-R intervals were compared in each group during the first parabola, the degree of variability of the R-R interval was smaller in the NKH477 group (n = 8) and greater in the vidarabine group (n = 8) than that in the control group (n = 8). In the eighth parabola (Fig. 3B), the degree of variability remained unchanged in the vidarabine group (n = 8), suggesting that adaptations to micro- and hypergravity were impaired in the vidarabine group (10, 23).

For further analysis, the R-R intervals under normogravity (phase I), microgravity (phase III), and hypergravity (phase IV) were plotted by time (s) versus R-R (ms) interval in each group during the first (Figs. 4A, 5A, 6A) and eighth parabolas (Figs. 4B, 5B, 6B). The R-R intervals under normogravity (phase I) during the first parabola were stable in each group (Fig. 4A), but became more variable during the eighth parabola. However, the degree of variability was greater in the vidarabine group and smaller in the NKH477 group than that in the control group (Fig. 4B).

Under microgravity (phase III), the degree of variability was less in the NKH477 group, as compared with the other groups (Fig. 5A). However, the degree of variability was greater in the vidarabine group (n = 8) and smaller in the NKH477 group (n = 9) than that in the control group (n = 8) during the eighth parabola (Fig. 5B).

Under hypergravity (phase IV), the degree of variability showed a similar tendency to that under microgravity in the three groups during the first (Fig. 6A) and the eighth parabolas (Fig. 6B).

Taken together, these results may indicate that pharmacological activation of AC5 stabilizes the R-R intervals not only under microgravity but also under hypergravity during parabolic flight.

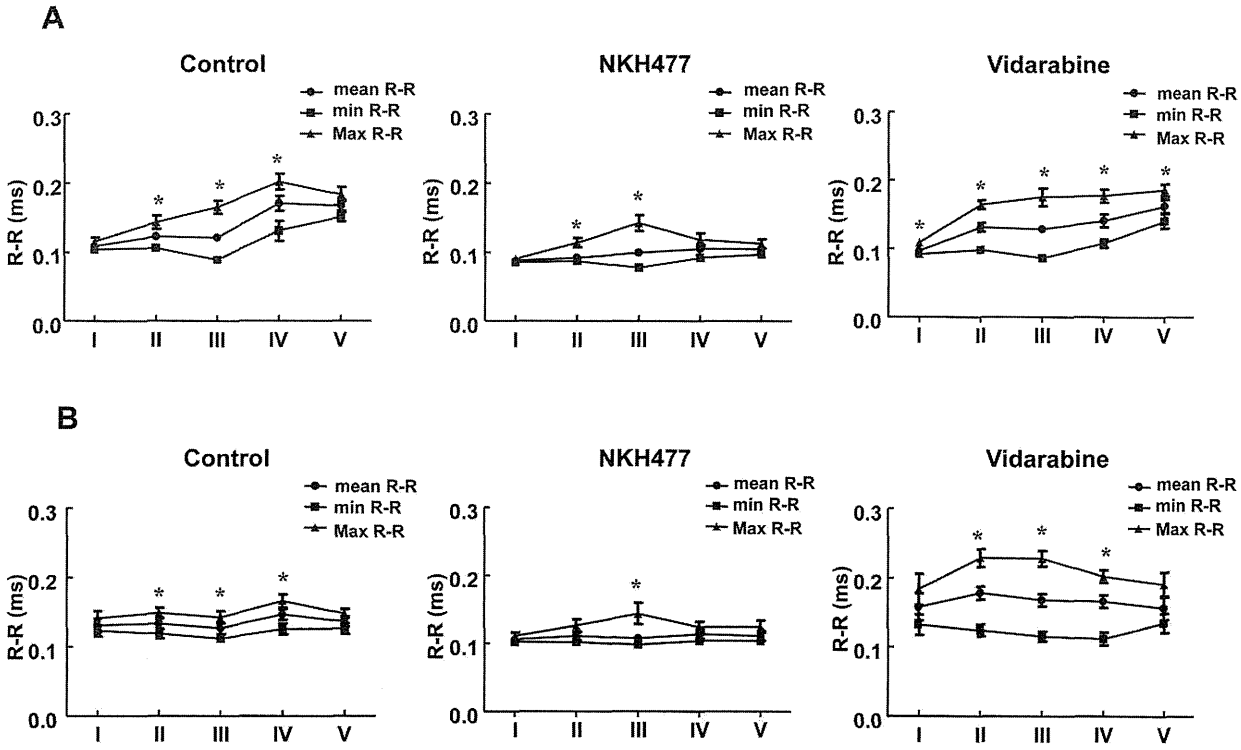

Fig. 3. Comparison of R-R interval during various phases of parabolic flights. Comparison of mean (mean), maximum (Max), and minimum (min) R-R intervals (ms) among phases I, II, III, IV, and V in the control (n = 8), NKH477 (n = 8 – 9), and vidarabine (n = 8) during the first parabola (A) and eighth parabola (B). Maximum R-R intervals were compared with the minimum R-R interval in each group (*$P < 0.05$).

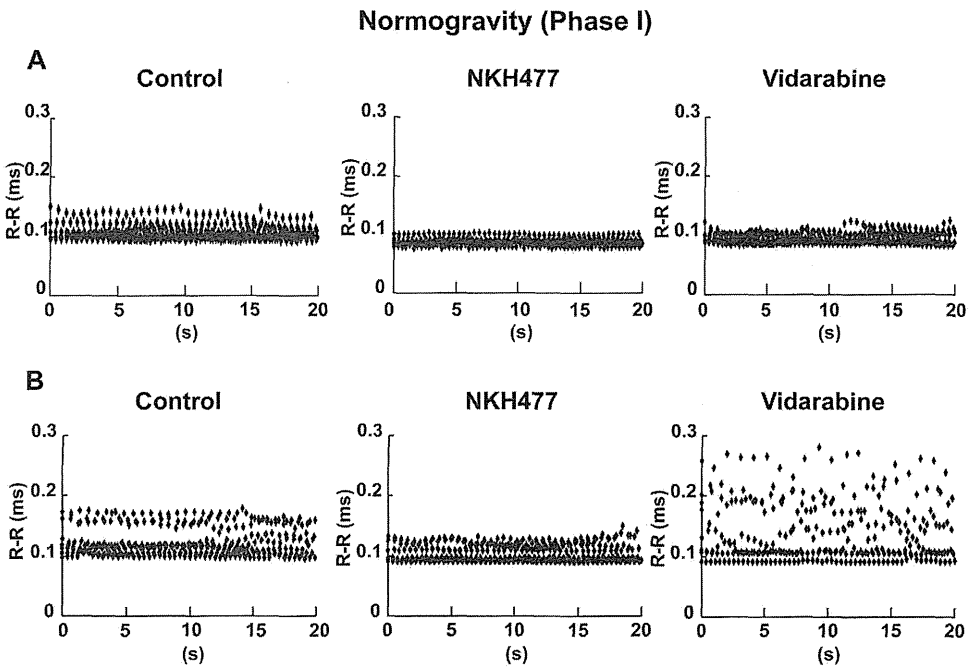

Fig. 4. Comparison of R-R interval under normogravity. R-R interval under normogravity (phase I) is shown by the plot of time (s) versus R-R interval (ms) in the control (n = 8), NKH477 (n = 8 – 9), vidarabine (n = 8) groups during the first (A) and eighth (B) parabolas.

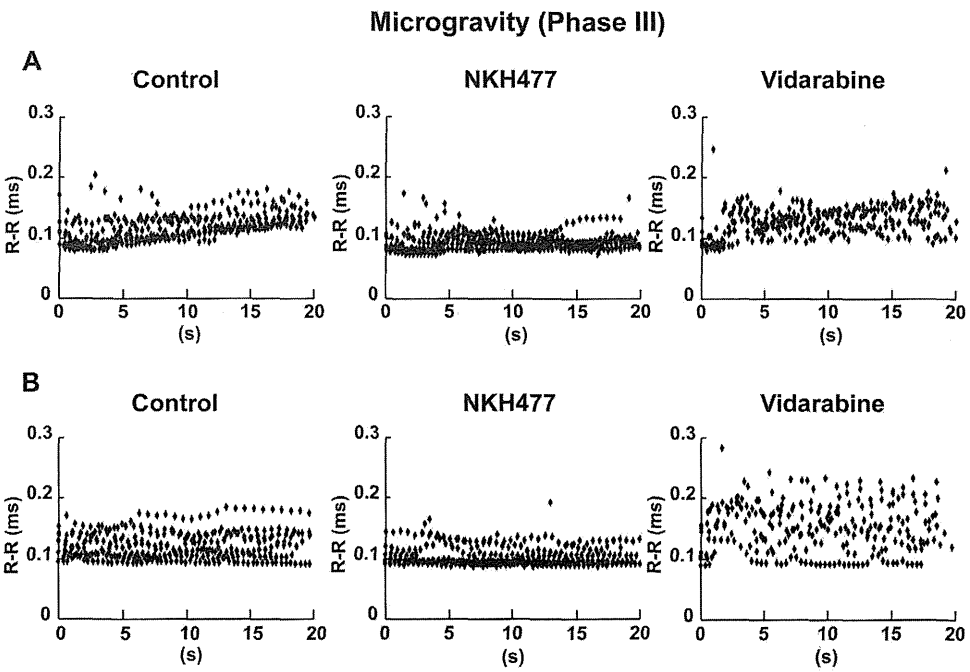

Fig. 5. Comparison of R-R interval under microgravity. Representative results under the microgravity (phase III) are shown by the plot of time (s) versus R-R interval (ms) in the control (n = 8), NKH477 (n = 8), and vidarabine (n = 8) groups during the first (A) and eighth (B) flights.

Effect of parabolic flight on SDNN of HRV

Because HR under gravitational stress is most likely regulated by the autonomic nervous system, we thus compared SDNN (Fig. 7A) and another parameter CV-SDNN (Fig. 7B) as a measure of total autonomic instability (24). SDNN and CV-SDNN were both significantly greater under microgravity (phase III) and hypergravity (phase II and IV) than those under normogravity (phase I) in each group. Notably, the absolute value of SDNN under microgravity (phase III) as well as hypergravity (phase IV) was strikingly greater in the vidarabine group (n = 8) and much smaller in the NKH477 group (n = 9) than that in the control group (n = 12). CV-SDNN showed similar behavior, indicating that increased AC5 activity stabilizes the autonomic control of the heart rate under gravitational stress.

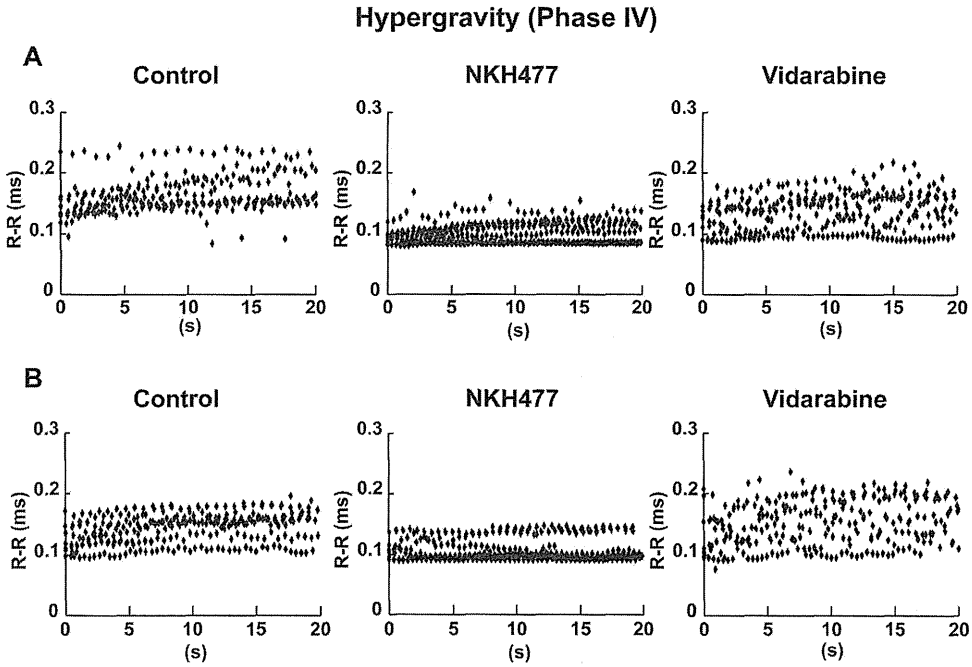

Fig. 6. Comparison of R-R interval under hypergravity. Representative results under the hypergravity (phase IV) are shown by the plot of time (s) versus R-R interval (ms) in the control (n = 8), NKH477 (n = 9), and vidarabine (n = 8) groups during the first (A) and eighth (B) flights.

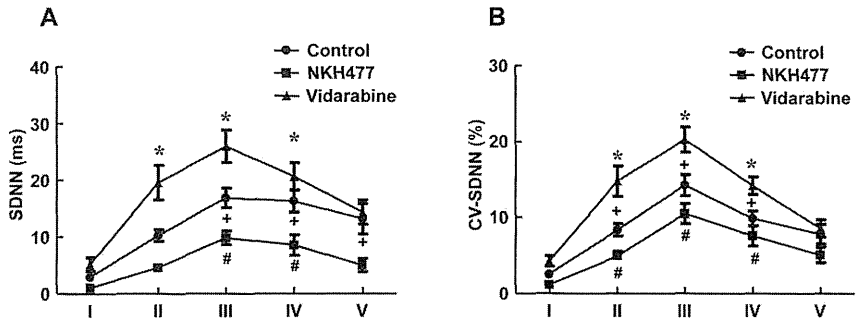

Fig. 7. Comparison of SDNN and CV-SDNN during parabolic flights. The standard deviation of normal R-R intervals (SDNN) (A) and coefficient of variation (CV, %) as a normalized index of SDNN (CV-SDNN) (B) during the first parabola. These indexes were compared between phase I and other phases in the control (n = 12), NKH477 (n = 9), and vidarabine (n = 8) groups ($^{+}$, *, $^{\#}P < 0.05$ vs. phase I).

Effect of parabolic flight on LF/HF of HRV

To further evaluate changes in autonomic nervous activity, we compared the ratio of LF to HF (LF/HF) in HRV analysis, an index of the sympathetic nervous tone in each phase of parabolic flight during the first parabola (16). When it was compared between normogravity (phase I) and microgravity (phase III), we found that LF/HF was significantly lower in phase I than that in phase III in the control and NKH477 groups (Fig. 8A) [control group (n = 10): phase I vs. phase III: 1.9 ± 0.4 vs. 0.9 ± 0.1 ms, $P < 0.05$; NKH477 group (n = 7): phase I vs. phase III, 2.1 ± 0.04 vs. 0.7 ± 0.05 ms, $P < 0.05$]. This was in agreement, at least in part, with previous studies in which decreased sympathetic nerve activity was demonstrated under microgravity in normal individuals (25). However, the vidarabine group did not show such a decrease [vidarabine group (n = 8): phase I vs. phase III: 1.9 ± 0.3 vs. 1.7 ± 0.3 ms, P = NS, not significant], suggesting that changes in sympathetic tone became small when AC5 activity was decreased with vidarabine.

Under hypergravity (phase IV), the ratio of LF/HF showed a similar tendency to that under microgravity in the three groups.

When it was compared between phase I (pre-parabolic flight) and phase V (post-parabolic flight), there was no difference in control group (phase I vs. phase V: 1.9 ± 0.4 vs. 1.7 ± 0.4 ms, P = NS) while it remained decreased in the NKH477 group (phase I vs. phase V: 2.1 ± 0.04 vs. 0.7 ± 0.1 ms, $P < 0.05$) (26). However, the vidarabine group showed no significant differences (phase I vs. phase V: 1.9 ± 0.3 vs. 1.9 ± 0.6 ms, P = NS).

Accordingly, sympathetic tone was transiently decreased under micro- and hypergravity in the control while it decreased in micro- and hypergravity and remained decreased in the NKH477 group even when gravity was normalized in the post-microgravity level flight (phase V); in contrast, such decreases were all ab-

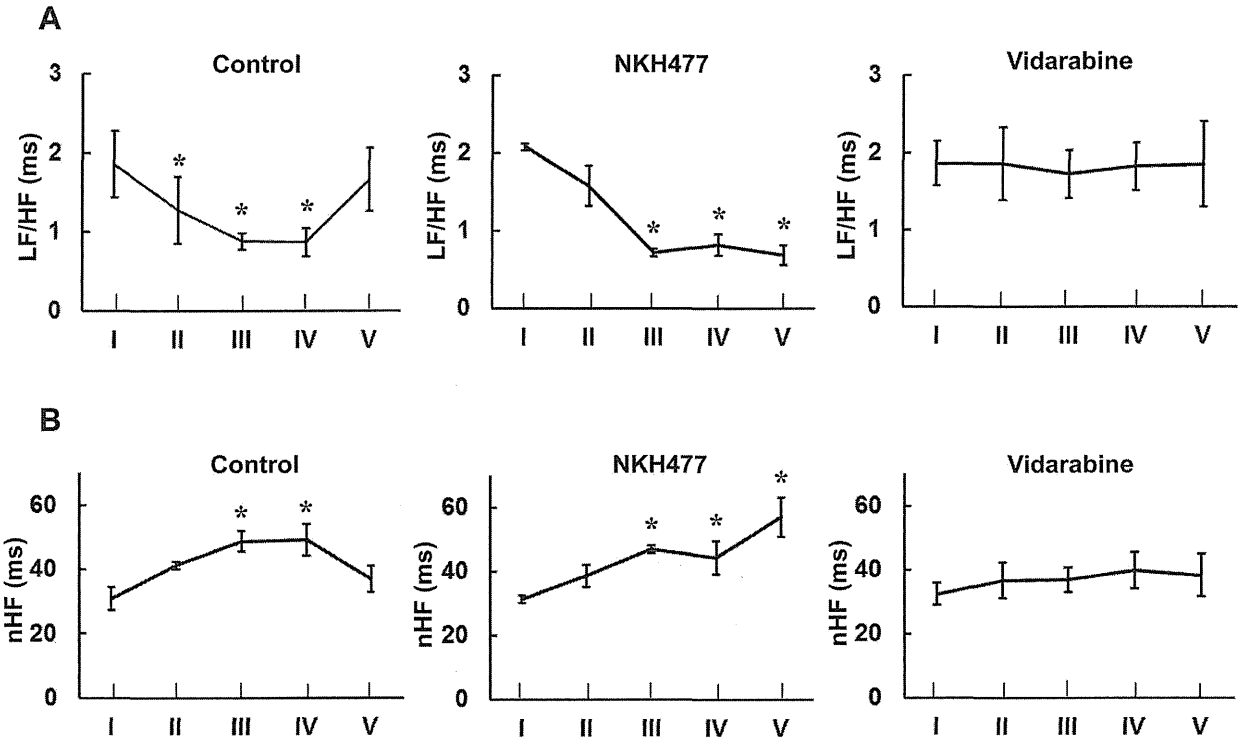

Fig. 8. Comparison of LF/HF and nHF during parabolic flights. A) LF/HF was compared as an index of sympathetic nerve activity in each phase during the first parabola in the control (n = 10), NKH477 (n = 7), and vidarabine (n = 8) groups (*$P < 0.05$ vs. phase I). B) nHF was compared as an index of parasympathetic nerve activity in each phase during the first parabola in control (n = 10), NKH477 (n = 7), and vidarabine (n = 8) groups (*$P < 0.05$ vs. phase I).

sent in the vidarabine group.

Effect of parabolic flight on nHF of HRV

HF power was normalized to account for differences in TP and was examined as an index of parasympathetic tone (16). When nHF was compared between normogravity (phase I) and microgravity (phase III), we found that it was significantly increased in microgravity in both the control and NKH477 groups (Fig. 8B) [control group (n = 10): phase I vs. phase III: 31 ± 3.6 vs. 49 ± 3.2 ms, $P < 0.05$; NKH477 group (n = 7): phase I vs. phase III: 31 ± 1.2 vs. 47 ± 1.2 ms, $P < 0.05$), suggesting that parasympathetic nerve tone was increased under microgravity in both the control and NKH477 groups. In contrast, there was no increase in nHF in the vidarabine group under microgravity (phase I vs. phase III: 32 ± 3.5 vs. 37 ± 3.8 ms, P = NS, n = 8), suggesting that microgravity-induced enhancement of parasympathetic nerve tone was attenuated in the vidarabine group.

Under hypergravity (phase IV), nHF showed a similar tendency to that under microgravity in the three groups.

nHF in post-microgravity (phase V) was returned to a similar level to that in pre-microgravity (phase I) in WT (37 ± 4.1 ms, P = NS), while it further increased in the NKH477 group (57 ± 6.2 ms, $P < 0.05$) (Fig. 8B). However, there were no such increases or decreases in the vidarabine group (38 ± 6.6 ms, P = NS).

Thus, parasympathetic nervous tone was transiently elevated in the control group, remained elevated in the NKH477 group, and showed no changes in the vidarabine group.

Taking these results together, in comparison to the control group, the NKH477 group showed continuous responses in the above autonomic (sympathetic and parasympathetic) parameters while the vidarabine group showed attenuated responses under micro- and hypergravity.

Discussion

Our current study demonstrated that activation of AC5 activity with NKH477 could stabilize HRV, while inhibition of AC5 with vidarabine could destabilize HRV under micro- and hypergravity during parabolic flight. Further, the absolute value of the total autonomic variability index (SDNN) was much greater in the vidarabine group than that in the control or NKH477 groups under microgravity as well as hypergravity. A marker of the sympathetic

nervous tone (LF/HF) was decreased to a greater degree in the NKH477 group relative to the control group, and a marker of parasympathetic tone (nHF) was instead increased to a greater degree in the NKH477 group; these changes were absent in the vidarabine group, indicating that pharmacological modulation of AC5 activity might be able to regulate the autonomic control of the heart rate under gravitational stress during parabolic flight.

AC consists of 9 mammalian transmembrane isoforms that differ in tissue distribution (3, 5), with type 6 AC (AC6) being the major fetal cardiac AC isoform, and AC5, the major cardiac isoform in adults (27, 28). All isoforms are stimulated by Gs, but AC5 and AC6 are the only Gi- and Ca^{2+}-inhibitable AC isoforms (3, 5). AC5 is responsible for at least one-third of the cardiac AC catalytic activity and plays an important role not only in sympathetic, but also parasympathetic cardiac function and heart rate without affecting Gi-gated K^+-channel current, which regulates normal pacing activity, as shown recently by us and others in AC5KO (7, 29). Overexpressing AC6 results in maintained basal HR (30), while overexpressing AC5 results in increased basal HR (13, 31), suggesting that AC5 may play an important role in regulating HR through the parasympathetic arm of the autonomic nervous system, as well as the sympathetic arm.

For many years, it has been recognized that many astronauts suffer from symptoms suggestive of autonomic dysfunction such as nausea, vomiting, and dizziness during the early days of space missions and their cardiovascular system subsequently adapts to the microgravity environment of space appropriately and effectively. However, on return to earth, from one-quarter to two-thirds of them have reduced orthostatic tolerance for a few weeks. The underlying molecular mechanisms remain unknown and are probably multifactorial, although alterations in the autonomic nervous system and/or neuromuscular function after spaceflight probably contribute to this problem (18, 19).

We have previously demonstrated that AC5 plays an important role in stabilizing HRV under microgravity, as well as hypergravity, during parabolic flight using genetically engineered mouse models (13). This present study has demonstrated that pharmacological activation/inhibition of AC5 activity can stabilize/destabilize the HRV not only under microgravity but also under hypergravity during parabolic flight. Importantly, NKH477 which was used in this study as a selective AC5 activator (NKH477) has been widely used for the treatment of acute heart failure in Japan since 1999. We will not need to wait for many years to get authorization for the use of NKH477 to treat autonomic dysfunction during and after space flight, if its usefulness is sufficiently confirmed by further studies.

There are plans for suborbital spaceflight or lunar tours for normal subjects as tourists, and also for prolonged space flight to Mars. It is also likely that not only astronauts, but also normal subjects will stay for up to several months in the international space station. Therefore, it is important to clarify the mechanism of the alterations in the autonomic nervous system and to develop suitable treatment. Our studies indicate that short-term, not long-term, pharmacological activation/inhibition of AC5 activity with NKH477 or vidarabine might rescue the autonomic dysfunction in the heart under microgravity in space and on earth after space flight, especially for untrained normal subjects.

Acknowledgments

This study was supported in part by grants from the Ministry of Health, Labor, and Welfare (Y.I.); the Kitsuen Kagaku Research Foundation (Y.I.); the Japanese Ministry of Education, Culture, Sports, Science, and Technology (Y.I., S.O., M.S., U.Y., R.K., Y.B., T.T., T.F.,Y.I.); Grant-in-Aid for Scientific Research on Innovative Areas (Y.I.); the Japan Space Forum (Y.I.); Takeda Science Foundation (Y.I., S.O., U.Y., M.S.); Yokohama Foundation for Advancement of Medical Science (S.O., U.Y., M.S., T.T., R.K.); Mitsubishi Pharma Research Foundation (S.O., M.S.); and Research for Promoting Technological Seeds A (discovery type) (S.O.); Yokohama Academic Foundation (S.O.); 2010 Commercialization Promotion Program for Biotechnology-related Studies (S.O.); Grant for Research and Development Project II (No. 8 and 14) of Yokohama City University (Y.I., S.O.); and Research Foundation for Community Medicine (S.O.).

References

1 Murray KJ, Reeves ML, England PJ. Protein phosphorylation and compartments of cyclic AMP in the control of cardiac contraction. Mol Cell Biochem. 1989;89:175–179.
2 Federman AD, Conklin BR, Schrader KA, Reed RR, Bourne HR. Hormonal stimulation of adenylyl cyclase through Gi-protein $\beta\gamma$ subunits. Nature. 1992;356:159–161.
3 Ishikawa Y, Homcy CJ. The adenylyl cyclases as integrators of transmembrane signal transduction. Circ Res. 1997;80:297–304.
4 Ishikawa Y. Regulation of cAMP signaling by phosphorylation. Adv Second Messenger Phosphoprotein Res. 1998;32:99–120.
5 Hanoune J, Defer N. Regulation and role of adenylyl cyclase isoforms. Annu Rev Pharmacol Toxicol. 2001;41:145–174.
6 Caulfield MP, Robbins J, Higashida H, Brown DA. Postsynaptic actions of acetylcholine: the coupling of muscarinic receptor subtypes to neuronal ion channels. Prog Brain Res. 1993;98: 293–301.
7 Okumura S, Kawabe J, Yatani A, Takagi G, Lee MC, Hong C, et al. Type 5 adenylyl cyclase disruption alters not only sympathetic but also parasympathetic and calcium-mediated cardiac regulation. Circ Res. 2003;93:364–371.
8 Okumura S, Takagi G, Kawabe J, Yang G, Lee MC, Hong C, et al. Disruption of type 5 adenylyl cyclase gene preserves cardiac function against pressure overload. Proc Natl Acad Sci

U S A. 2003;100:9986–9990.
9 Okumura S, Vatner DE, Kurotani R, Bai Y, Gao S, Yuan Z, et al. Disruption of type 5 adenylyl cyclase enhances desensitization of cyclic adenosine monophosphate signal and increases Akt signal with chronic catecholamine stress. Circulation. 2007;116:1776–1783.
10 Di Rienzo M, Castiglioni P, Iellamo F, Volterrani M, Pagani M, Mancia G, et al. Dynamic adaptation of cardiac baroreflex sensitivity to prolonged exposure to microgravity: data from a 16-day spaceflight. J Appl Physiol. 2008;105:1569–1575.
11 Abe C, Tanaka K, Awazu C, Morita H. Impairment of vestibular-mediated cardiovascular response and motor coordination in rats born and reared under hypergravity. Am J Physiol Regul Integr Comp Physiol. 2008;295:R173–R180.
12 Iwasaki K, Shiozawa T, Kamiya A, Michikami D, Hirayama K, Yajima K, et al. Hypergravity exercise against bed rest induced changes in cardiac autonomic control. Eur J Appl Physiol. 2005;94:285–291.
13 Okumura S, Tsunematsu T, Bai Y, Qian J, Ono S, Suzuki S, et al. Type 5 adenylyl cyclase plays a major role in stabilizing heart rate in response to microgravity induced by parabolic flight. J Appl Physiol. 2008;105:173–179.
14 Toya Y, Schwencke C, Ishikawa Y. Forskolin derivatives with increased selectivity for cardiac adenylyl cyclase. J Mol Cell Cardiol. 1998;30:97–108.
15 Iwatsubo K, Minamisawa S, Tsunematsu T, Nakagome M, Toya Y, Tomlinson JE, et al. Direct inhibition of type 5 adenylyl cyclase prevents myocardial apoptosis without functional deterioration. J Biol Chem. 2004;279:40938–40945.
16 Malik M, Bigger JT, Camm AJ, Kleiger RE, Malliani A, Moss AJ, et al; Task force of the European society of cardiology and the north American society of pacing and electrophysiology. Heart rate variability. Standards of measurement, physiological interpretation, and clinical use. Eur Heart J. 1996;17:354–381.
17 Young LR, Oman CM, Watt DG, Money KE, Lichtenberg BK. Spatial orientation in weightlessness and readaptation to earth's gravity. Science. 1984;225:205–208.
18 Buckey JC Jr, Lane LD, Levine BD, Waterpaugh DE, Wright SJ, Moore WE, et al. Orthostatic intolerance after spaceflight. J Appl Physiol. 1996;81:7–18.
19 Fritsch-Yelle JM, Whitson PA, Bondar RL, Brown TE. Subnormal norepinephrine release relates to presyncope in astronauts after spaceflight. J Appl Physiol. 1996;81:2134–2141.
20 Seps B, Beckers F, Aubert AE. Heart rate variability during gravity transitions. Comput Cardiol. 2002;29:433–436.
21 Gehrmann J, Berul CI. Cardiac electrophysiology in genetically engineered mice. J Cardiovasc Electrophysiol. 2000;11:354–368.
22 Tepe NM, Liggett SB. Transgenic replacement of type V adenylyl cyclase identifies a critical mechanism of β-adrenergic receptor dysfunction in the Gαq overexpressing mouse. FEBS Lett. 1999;458:236–240.
23 Levine BD, Pawelczyk JA, Ertl AC, Coz JF, Zuckermann JH, Diedrich A, et al. Human muscle sympathetic neural and haemodynamic responses to tilt following spaceflight. J Physiol. 2002;538:331–340.
24 Kamen PW, Krum H, Tonkin AM. Poincare plot of heart rate variability allows quantitative display of parasympathetic nervous activity in humans. Clin Sci (Lond). 1996;91:201–208.
25 Migeotte PF, Prisk GK, Paiva M. Microgravity alters respiratory sinus arrhythmia and short-term heart rate variability in humans. Am J Physiol Heart Circ Physiol. 2003;284:H1995–H2006.
26 Verheyden B, Beckers F, Aubert AE. Spectral characteristics of heart rate fluctuations during parabolic flight. Eur J Appl Physiol. 2005;95:557–568.
27 Tobise K, Ishikawa Y, Holmer SR, Im MJ, Newell JB, Yoshine H, et al. Changes in type VI adenylyl cyclase isoform expression correlate with a decreased capacity for cAMP generation in the aging ventricle. Circ Res. 1994;74:596–603.
28 Espinasse I, Iourgenko V, Defer N, Salmon F, Hanoune J, Mercadier JJ. Type V, but not type VI, adenylyl cyclase mRNA accumulates in the rat heart during ontogenic development. Correlation with increased global adenylyl cyclase activity. J Mol Cell Cardiol. 1995;27:1789–1795.
29 Tang T, Lai NC, Roth DM, Drumm J, Guo T, Lee KW, et al. Adenylyl cyclase type V deletion increases basal left ventricular function and reduces left ventricular contractile responsiveness to β-adrenergic stimulation. Basic Res Cardiol. 2006;101:117–126.
30 Gao MH, Lai NC, Roth DM, Zhou J, Zhu J, Anza T, et al. Adenylylcyclase increases responsiveness to catecholamine stimulation in transgenic mice. Circulation. 1999;99:1618–1622.
31 Tepe NM, Lorenz JN, Yatani A, Dash R, Kranias EG, Dorn GW II, et al. Altering the receptor-effector ratio by transgenic overexpression of type V adenylyl cyclase: enhanced basal catalytic activity and function without increased cardiomyocyte β-adrenergic signalling. Biochemistry. 1999;38:16706–16713.

Type 5 Adenylyl Cyclase Increases Oxidative Stress by Transcriptional Regulation of Manganese Superoxide Dismutase via the SIRT1/FoxO3a Pathway

Lo Lai, PhD; Lin Yan, PhD; Shumin Gao, MD, PhD; Che-Lin Hu, PhD; Hui Ge, BS, Amy Davidow, PhD; Misun Park, PhD; Claudio Bravo, MD; Kousaku Iwatsubo, MD, PhD; Yoshihiro Ishikawa, MD; Johan Auwerx, MD, PhD; David A. Sinclair, PhD; Stephen F. Vatner, MD; Dorothy E. Vatner, MD

Background—For reasons that remain unclear, whether type 5 adenylyl cyclase (AC5), 1 of 2 major AC isoforms in heart, is protective or deleterious in response to cardiac stress is controversial. To reconcile this controversy we examined the cardiomyopathy induced by chronic isoproterenol in AC5 transgenic (Tg) mice and the signaling mechanisms involved.

Methods and Results—Chronic isoproterenol increased oxidative stress and induced more severe cardiomyopathy in AC5 Tg, as left ventricular ejection fraction fell 1.9-fold more than wild type, along with greater left ventricular dilation and increased fibrosis, apoptosis, and hypertrophy. Oxidative stress induced by chronic isoproterenol, detected by 8-OhDG was 15% greater, P=0.007, in AC5 Tg hearts, whereas protein expression of manganese superoxide dismutase (MnSOD) was reduced by 38%, indicating that the susceptibility of AC5 Tg to cardiomyopathy may be attributable to decreased MnSOD expression. Consistent with this, susceptibility of the AC5 Tg to cardiomyopathy was suppressed by overexpression of MnSOD, whereas protection afforded by the AC5 knockout (KO) was lost in AC5 KO×MnSOD heterozyous KO mice. Elevation of MnSOD was eliminated by both sirtuin and MEK inhibitors, suggesting both the SIRT1/FoxO3a and MEK/ERK pathway are involved in MnSOD regulation by AC5.

Conclusions—Overexpression of AC5 exacerbates the cardiomyopathy induced by chronic catecholamine stress by altering regulation of SIRT1/FoxO3a, MEK/ERK, and MnSOD, resulting in oxidative stress intolerance, thereby shedding light on new approaches for treatment of heart failure. (***Circulation.*** **2013;127:1692–1701.)**

Key Words: adenylyl ■ adrenergic receptors ■ cardiomyopathies ■ oxidative stress

Adenylyl cyclase (AC) is a key regulator of health and longevity in organisms ranging from yeast to mammals.[1–5] In the heart AC is a critical link in sympathetic control and beta adrenergic receptor (β-AR) signaling and therefore plays a fundamental role in mediating not only baseline cardiac function, but also the cardiac response to stress (eg, in the pathogenesis of heart failure). Type 5 AC (AC5) is 1 of 2 major isoforms in heart, the other being type 6 AC (AC6). For reasons that remain unclear, whether AC5 is protective or deleterious in response to cardiac stress is controversial, particularly with respect to the signaling mechanisms involved, and whether these mechanisms are shared by AC6. It is generally accepted that cardiac-specific AC5 overexpressed (AC5 transgenic [Tg]) mice exhibit enhanced cardiac performance,[6] which follows from the role of AC, which generates cAMP on β-AR stimulation resulting in increased cardiac contractility and heart rate. However, the extent to which altered AC5 regulation is protective with chronic stress remains controversial. Previous studies examined whether overexpression or disruption of AC5 in the heart could affect the progression of cardiomyopathy induced by overexpression of Gαq and β1-AR. This was accomplished by mating overexpressed Gαq and β1-AR with AC5 Tg or AC5 knockout (KO) mice. These studies found that AC5 Tg rescued Gαq cardiomyopathy,[6] but not β1-AR cardiomyopathy,[7] and AC5 KO mice failed to rescue cardiomyopathy in Gαq mice.[8] In addition, AC5 KO mice rescued cardiomyopathies from chronic pressure overload,[9] chronic catecholamine stress,[10] and aging.[1]

Clinical Perspective on p 1701

Because β-AR signaling, of which AC is central, plays a key role in the pathogenesis of heart failure and because β-AR blockade therapy is widely used in patients with heart failure, but that therapy is still far from perfect, it becomes

Received August 6, 2012; accepted March 14, 2013.

From the Department of Cell Biology and Molecular Medicine and Cardiovascular Research Institute, New Jersey Medical School, University of Medicine and Dentistry of New Jersey, Newark, NJ (L.L., LY., S.G., C.-L.H., H.G., A.D., M.P., C.B., K.I., Y.I., S.F.V., D.E.V.); Glenn Laboratories for the Biological Mechanisms of Aging, Department of Genetics, Harvard Medical School, Boston, MA (D.A.S.); and the Laboratory of Integrative and Systems Physiology, Ecole Polytechnique Fédérale de Lausanne, CH-1015 Lausanne, Switzerland (J.A.).

Guest Editor for this article was Danial Bernstein, MD.

The online-only Data Supplement is available with this article at http://circ.ahajournals.org/lookup/suppl/doi:10.1161/CIRCULATIONAHA.112.001212/-/DC1.

Correspondence to Dorothy E. Vatner, MD, Department of Cell Biology & Molecular Medicine, University of Medicine & Dentistry of New Jersey, New Jersey Medical School, 185 South Orange Avenue, MSB G609, Newark, NJ 07103. E-mail vatnerdo@umdnj.edu

Circulation **is available at http://circ.ahajournals.org** **DOI: 10.1161/CIRCULATIONAHA.112.001212**

critical to reconcile the controversy and understand the role of AC in the heart in the development of cardiomyopathy and heart failure, which would eventually be of clinical importance. Accordingly, this was the overall goal of the current investigation. We first examined the extent to which manganese superoxide dismutase (MnSOD) regulation and oxidative stress were altered in AC5 Tg at baseline and in response to chronic β-AR stimulation, because it is known that β-AR stimulation increases oxidative stress,[11,12] and that MnSOD is upregulated in AC5 KO mice.[1] The results of the experiments with bigenic mice (AC5 Tg×MnSOD Tg and AC5 KO×MnSOD$^{+/-}$) led us to elucidate the signaling mechanisms linking AC5, MnSOD, and oxidative stress and the involvement of the Sirtuin 1/Forkhead box O3 (SIRT1/FoxO3a) pathway. The SIRT1/FoxO3a pathway was selected to investigate, because MnSOD is upregulated in the AC5 KO mouse, which lives longer than wild type (WT),[1] and FoxO3a is the transcriptional factor most closely related to the antioxidative protective effects associated with longevity, as shown in several models: *C elegans*,[13,14] rats,[15] and human quiescent cells.[16] The final goal was to investigate whether this pathway is regulated specifically by AC5, or whether it is common to all AC signaling in the heart, which would mean that these mechanisms were shared by the other major cardiac AC isoform, AC6.

Methods

Mouse Models

Generation of AC5 Tg mice was described previously.[17] AC5 KO×MnSOD$^{+/-}$ mice were generated by crossing AC5 KO mice with MnSOD heterozygous mice. AC5 Tg×MnSOD Tg were generated by crossing AC5 Tg mice with MnSOD Tg mice (from Jackson Laboratory, Bar Harbor, ME; Stock ID, 009438). To produce catecholamine cardiomyopathy, isoproterenol (ISO) was delivered to 3- to 5-month-old Tg mice, bigenic mice, and corresponding control littermates for 7 days at a dose of 60 mg/kg/d with a miniosmotic pump (ALZET model 2001, DURECT Corp, Cupertino, CA) as described.[10] The severity of the cardiomyopathy was assessed by echocardiographic measurements of left ventricular (LV) ejection fraction and LV end diastolic and end systolic diameter and histopathological measurements of myocardial fibrosis, apoptosis, and myocyte cross sectional area. For the Tempol treatment group, 4-hydroxy-2,2,6,6-tetramethyl-piperidine-1-oxyl (Tempol, Sigma) was administered to AC5 Tg mice by dissolving it in drinking water at a concentration of 1 mmol/L for 1 month before chronic ISO infusion to block oxidative stress. Animals used in this study were maintained in accordance with the *Guide for the Care and Use of Laboratory Animals* (National Research Council, Eighth Edition 2011). This study was approved by the Animal Care and Use Committee at New Jersey Medical School.

Experimental Procedures

All techniques are described in more detail in the online-only Data Supplement with references to previous work with these techniques. Experimental procedures included the following: adenoviral construction (Figure II in the online-only Data Supplement), physiological studies,[10] primary culture of neonatal rat ventricular myocytes,[18] AC assay,[10] immunoprecipitation, Western blotting,[1] quantitative RT-PCR,[18] 8-hydroxy-2′-deoxyguanosine (8-OHdG) ELISA assay, chemiluminescent assay for superoxide production,[19] subcellular fractionation, luciferase activity, Chromatin Immunoprecipitation (ChIP) assay,[15] and histological analyses (apoptosis, fibrosis, and cell size).[20]

Statistical Analysis

Normally distributed data were presented as mean±SEM. Otherwise, data were summarized using the Median and range. When the data were normally distributed, we used Student unpaired *t* test to compare 2 independent groups; otherwise, the difference was tested using the Mann–Whitney *U* test. For a comparison of ≥3 groups, 1-way ANOVA was used if the sample population was normally distributed and within-group variances were approximately equal. The Student-Newman-Keuls test was used for post hoc analysis. For data that did not meet the ANOVA assumptions, the Kruskal–Wallis test was applied and post hoc testing was carried out using the Mann–Whitney *U* test with Bonferroni correction. The Bonferroni correction factor is 3 for Figures 1, 5F, and 5G. GraphPad-Prism 5.0 (GraphPad-Software, San Diego, CA), SPSS 20.0 (SPSS Inc, Chicago, IL), and SAS 9.3 (SAS, Research Triangle, NC) were used to perform the statistical analyses. *P* values <0.05 defined statistical significance.

Results

AC5 Tg Mouse Model and Cardiomyopathy Induced by Chronic Isoproterenol

AC5 protein expression, assessed by Western blot analysis, was increased 26-fold in AC5 Tg (Figure IA in the online-only Data Supplement). Basal AC activity was increased 13-fold in AC5 Tg mice hearts compared to WT, and was increased 10-fold with forskolin compared to WT (Figure IB in the online-only Data Supplement). The AC5 Tg exhibited increased LV ejection fraction (LVEF), P=0.0009, without ISO (WT=73 [67–74]%; AC5 Tg=78 [75–81] %) and heart rate was not significantly different, P=0.3176, (WT=337 [325–465] bpm; AC5 Tg= 442 [355–500] bpm). The increase in LVEF in response to an ISO challenge was similar in AC5 Tg and WT mice (Figure IC in the online-only Data Supplement).

Chronic ISO infusion induced more severe cardiomyopathy in AC5 Tg compared with WT (ie, LVEF was lower), P=0.0058, in AC5 Tg (45 [30–49] %) compared with WT (54 [47–58] %). Actually, the decline in LVEF was even more significant, because that takes into account the different baseline levels where LVEF was higher in AC5 Tg and fell to a lower level, P=0.0021 (Figure 1A). In addition, the LV dilated more in AC5 Tg mice than WT (Table I in the online-only Data Supplement). Similarly, chronic ISO induced more fibrosis (2.0-fold) and more myocyte apoptosis (2.8-fold) in AC5 Tg mice compared with WT (Figure 1B and 1C). There was also more LV hypertrophy, as measured by myocyte cross sectional area, but the increase (1.2-fold) was not as great as with fibrosis and apoptosis.

Overexpression of AC5 Increased Oxidative Stress

After chronic ISO stimulation, AC5 Tg mice exhibited 19% more glutathione disulfide (GSSG) content, an indicator of oxidative stress, than WT littermates (Figure 2A). Consistent with this, AC5 Tg mice had 15% more oxidative stress–induced DNA damage compared with WT mice after chronic ISO stimulation detected by 8-OHdG ELISA (Figure 2B). In AC5 overexpressed neonatal myocytes, superoxide production was approximately 2-fold more than in the control group (Figure 2C). AC5 knockdown (KD) myocytes increased cell survival with H_2O_2 treatment (Figure 2D). MnSOD is part of a mechanism that might be responsible for the opposite response of AC5 overexpressed (OE) and AC5 KD toward oxidative stress, because MnSOD is upregulated in AC5 KO mice.